

## Symbiosis at its limits: ecophysiological consequences of lichenization in the genus *Prasiola* in Antarctica

Beatriz Fernández-Marín<sup>1,8,\*</sup>, Marina López-Pozo<sup>1</sup>, Alicia V. Perera-Castro<sup>2</sup>, Miren Irati Arzac<sup>1</sup>, Ana Sáenz-Ceniceros<sup>1</sup>, Claudia Colesie<sup>3</sup>, Asunción de los Ríos<sup>4</sup>, Leo G. Sancho<sup>5</sup>, Ana Pintado<sup>5</sup>, José M. Laza<sup>6</sup>, Sergio Pérez-Ortega<sup>7</sup> and José I. García-Plazaola<sup>1</sup>

<sup>1</sup>Department of Plant Biology and Ecology, University of the Basque Country (UPV/EHU), Barrio Sarriena sn, 48940 Leioa, Spain, <sup>2</sup>Research Group on Plant Biology under Mediterranean Conditions, Universitat de les Illes Balears (UIB) - Instituto de Investigaciones Agroambientales y de Economía del Agua (INAGEA), Carretera de Valldemossa Km 7.5, 07122, Palma, Illes Balears, Spain, <sup>3</sup>Global Change Institute, School of GeoSciences, University of Edinburgh, Alexander Crum Brown Road, Edinburgh EH9 3FF, UK, <sup>4</sup>Museo Nacional de Ciencias Naturales (MNCN-CSIC), Serrano 115 dpdo, 28006 Madrid, Spain, <sup>5</sup>Botany Section, Fac. Farmacia, Universidad Complutense, 28040 Madrid, Spain, <sup>6</sup>Laboratory of Macromolecular Chemistry (Labquimac), Department of Physical Chemistry, University of the Basque Country (UPV/EHU), Barrio Sarriena sn, 48940 Leioa, Spain, <sup>7</sup>Real Jardín Botánico (RJB-CSIC), Plaza de Murillo 2, 28014 Madrid, Spain and <sup>8</sup>Department of Botany, Ecology and Physiology, University of La Laguna (ULL), 38200 La Laguna, Canarias, Spain

\*For correspondence. E-mail [beatriz.fernandezm@ehu.es](mailto:beatriz.fernandezm@ehu.es)

Received: 16 January 2019 Returned for revision: 2 April 2019 Editorial decision: 6 September 2019 Accepted: 13 September 2019  
Published electronically 24 September 2019

- **Background and Aims** Lichens represent a symbiotic relationship between at least one fungal and one photosynthetic partner. The association between the lichen-forming fungus *Mastodia tessellata* (Verrucariaceae) and different species of *Prasiola* (Trebouxiophyceae) has an amphipolar distribution and represents a unique case study for the understanding of lichen symbiosis because of the macroalgal nature of the photobiont, the flexibility of the symbiotic interaction and the co-existence of free-living and lichenized forms in the same microenvironment. In this context, we aimed to (1) characterize the photosynthetic performance of co-occurring populations of free-living and lichenized *Prasiola* and (2) assess the effect of the symbiosis on water relations in *Prasiola*, including its tolerance of desiccation and its survival and performance under sub-zero temperatures.
- **Methods** Photochemical responses to irradiance, desiccation and freezing temperature and pressure–volume curves of co-existing free-living and lichenized *Prasiola* thalli were measured *in situ* in Livingston Island (Maritime Antarctica). Analyses of photosynthetic pigment, glass transition and ice nucleation temperatures, surface hydrophobicity extent and molecular analyses were conducted in the laboratory.
- **Key Results** Free-living and lichenized forms of *Prasiola* were identified as two different species: *P. crispa* and *Prasiola* sp., respectively. While lichenization appears to have no effect on the photochemical performance of the alga or its tolerance of desiccation (in the short term), the symbiotic lifestyle involves (1) changes in water relations, (2) a considerable decrease in the net carbon balance and (3) enhanced freezing tolerance.
- **Conclusions** Our results support improved tolerance of sub-zero temperature as the main benefit of lichenization for the photobiont, but highlight that lichenization represents a delicate equilibrium between a mutualistic and a less reciprocal relationship. In a warmer climate scenario, the spread of the free-living *Prasiola* to the detriment of the lichen form would be likely, with unknown consequences for Maritime Antarctic ecosystems.

**Key words:** Abiotic stress, alga, desiccation tolerance, freezing tolerance, glassy state, lichen, *Mastodia tessellata*, photobiont, photoprotection, photosynthesis, polar, *Turgidosculum*.

### INTRODUCTION

Lichens are symbiotic organisms resulting from the association of one fungal and at least one photosynthetic partner (mycobiont and photobiont, respectively). They can thrive in some of the harshest environments on Earth, such as drylands and tundra (e.g. Antarctica). As an illustrative example of their relevance, the current Antarctic flora includes more than 350 species of lichens, around 130 species of bryophytes (100–115 mosses and 27 liverworts) and only two species of tracheophytes (Kappen, 2000; Øvstedal and Lewis Smith, 2001; Peat *et al.*, 2007; Ochrya

*et al.*, 2008). Lichens play essential roles in primary production and nutrient cycling in diverse ecosystems (Asplund and Wardle, 2017), including polar regions, where they represent a large fraction of the local biodiversity. Hence, the understanding of the ecophysiology of lichens as primary producers is of crucial relevance. With regard to climate change scenarios, lichens receive increasing attention, with particular emphasis on more vulnerable environments such as drylands and polar habitats (Laguna-Defior *et al.*, 2016; Bao *et al.*, 2018; Colesie *et al.*, 2018; Ladrón de Guevara *et al.*, 2018). In this sense, different manipulative

experiments have recently indicated that: (1) increasing temperatures may alter lichen communities in drylands (Ladrón de Guevara *et al.*, 2018) and the Antarctic (Colesie *et al.*, 2018), (2) a higher frequency of freezing/thawing events during winter may have a negative impact on Arctic and Antarctic lichens (Harańczyk *et al.*, 2003; Bjerke, 2011), and (3) a prolonged period under snow may threaten lichen subsistence in Maritime Antarctica (Bokhorst *et al.*, 2016; Sancho *et al.*, 2017).

Lichens are poikilohydric organisms and, the vast majority of the species are considered to be tolerant of desiccation, i.e. able to withstand extremely low cellular water contents [ $<0.1 \text{ g H}_2\text{O g}^{-1}$  dry weight (DW)] and to reactivate metabolic activity upon rehydration (Kranner *et al.*, 2008). Thus, very finely tuned physiological and biochemical processes, related mainly to photochemical and antioxidant protection, seem to be key aspects of their capacity to deal with severe cell dehydration (Kranner, 2002; Heber *et al.*, 2007; Fernández-Marín *et al.*, 2010). In dry lichens, a particular quenching of chlorophyll (Chl) fluorescence relates to the efficient dissipation of light energy during dry periods (Veerman *et al.*, 2007; Heber *et al.*, 2010). Among antioxidants, zeaxanthin and glutathione seem to play a major role in the preservation of chloroplast and cell functionality during desiccation/rehydration cycles (Kranner *et al.*, 2003; Fernández-Marín *et al.*, 2010). Only recently, the loss of cell turgor has been pointed out as a relevant sensor and a trigger of desiccation-tolerance responses (Banchi *et al.*, 2018), and the physiology of their water relations is just starting to be addressed from an irreversible thermodynamics approach, e.g. by measuring water potential isotherms (Nardini *et al.*, 2013; Petruzzellis *et al.*, 2018). Other physiochemical consequences of desiccation, such as entering into the so-called glassy state, which severely limits biochemical reactions in desiccation-tolerant mosses and tracheophytes (Fernández-Marín *et al.*, 2013, 2018b), remain unexplored in lichens so far.

Albeit lichens dominate cold environments and although desiccation and low temperatures lead to many similar physiological consequences in photosynthetic cells (Fernández-Marín *et al.*, 2018b; Verhoeven *et al.*, 2018), their tolerance of freezing has been greatly understudied in lichens in comparison with other organisms (Bjerke, 2011; Nowak *et al.*, 2018). This may be because (1) as poikilohydric organisms lichens are assumed to withstand low temperatures when dry (Gauslaa and Solhaug, 1999) and (2) some species (from boreo-alpine and polar regions, mainly) are capable of C assimilation at sub-zero temperatures (Kappen and Lange, 1972; Kappen, 1989; Barták *et al.*, 2007). Recent work, however, has shown great variability in the sensitivity of lichen species to freezing when wet and have evidenced an important gap in our knowledge regarding the physiological and molecular aspects involved in it (Bjerke, 2011; Hájek *et al.*, 2016; Nowak *et al.*, 2018; Solhaug *et al.*, 2018). Although the molecular mechanisms of frost and desiccation tolerances are not fully understood in lichens (Nowak *et al.*, 2018), several studies have pointed out that the symbiosis is beneficial to the photobiont by counteracting desiccation (Kranner *et al.*, 2005; Kosugi *et al.*, 2009), while others have highlighted the capability of the free-living photobiont to withstand low temperature and/or desiccation, particularly within the genus *Trebouxia* (Sadowsky and Ott, 2012; Candotto Carniel *et al.*, 2015).

Overall, the complex relationships among the components of the lichen consortium hinder the understanding of their separate physiologies and thus of the physiological consequences of the symbiosis for the individual partners. Until now, major advances in their understanding are a result of studying isolated symbionts cultured under laboratory conditions. Valuable information has been obtained through this approach regarding different aspects of photobiont ecophysiology, e.g. cell osmolarity (Kosugi *et al.*, 2014), nutrient uptake (Pavlova *et al.*, 2017), photochemistry (Guéra *et al.*, 2016) and, more recently, water relations (Centeno *et al.*, 2016; Banchi *et al.*, 2018). Field studies would still be needed to completely understand the ecophysiology of lichen photobionts in their free-living forms. Nevertheless, their sparse presence in the environment and the fact that they usually cohabit with many other taxa of microflora [e.g. on the surface of other lichen species' thalli (Muggia *et al.*, 2013)] make the study of free-living photobionts an extremely challenging task under natural conditions.

A unique opportunity, though, arises from the study of the exceptional association established by the lichen-forming fungus *Mastodia tessellata* (Verrucariaceae) and its photobiont, a green alga of the genus *Prasiola* (Prasiolales, Trebouxiophyceae). Two main reasons for this are (1) the macroscopic and multicellular nature of the photobiont, the only known case, together with *Turgidosculum ulvae*, of a fungus forming a lichen symbiosis with a blade-like alga (Pérez-Ortega *et al.*, 2018), and (2) the apparent coexistence of free-living and lichenized forms of *Prasiola* in the same microenvironments (Huiskes *et al.*, 1997a) (see also Fig. 1). The characteristic symbiosis formed by *M. tessellata* has repeatedly attracted the attention of the scientific community. The species occurs in the upper littoral zone at high latitudes of both hemispheres, with extant populations in Alaska (USA), British Columbia (Canada), Tierra del Fuego (Chile), New Zealand, Tasmania (Australia), Antarctica and the sub-Antarctic islands (for a more detailed distribution area see Garrido-Benavent *et al.*, 2018). Pérez-Ortega *et al.* (2010) studied the phylogenetic affinities of both symbionts, and dismantled the monotypic family Mastodiaceae, showing that *M. tessellata* is closely related to marine members of the family Verrucariaceae. These authors also thoroughly characterized the interactions between the two symbionts at the ultrastructural level, revealing a particular kind of fungal haustorium not previously observed, and pointing to a relationship that was not parasitic but rather a dynamic equilibrium in which the photobiont can occasionally escape from the mycobiont. More recently, it has been shown that there are more than one species of *Prasiola* algae forming lichen symbioses with *M. tessellata* (Garrido-Benavent *et al.*, 2017). The known bipolar distribution of the lichen-forming fungus and its photobionts is the result of a complex of past events, with relatively recent joint dispersal from the southern hemisphere to the northern hemisphere (Garrido-Benavent *et al.*, 2018).

To the best of our knowledge, *in situ* comparison (in Antarctica) of free-living versus lichenized *Prasiola* (e.g. *M. tessellata*) has only been done before by Huiskes *et al.* (1997a). Huiskes and co-workers showed that subjection to prolonged hydration was detrimental to the photosynthetic rates of the lichen but not of the free-living *Prasiola* specimens (Huiskes *et al.*, 1997a). With a broad combination of methodologies and by integrating

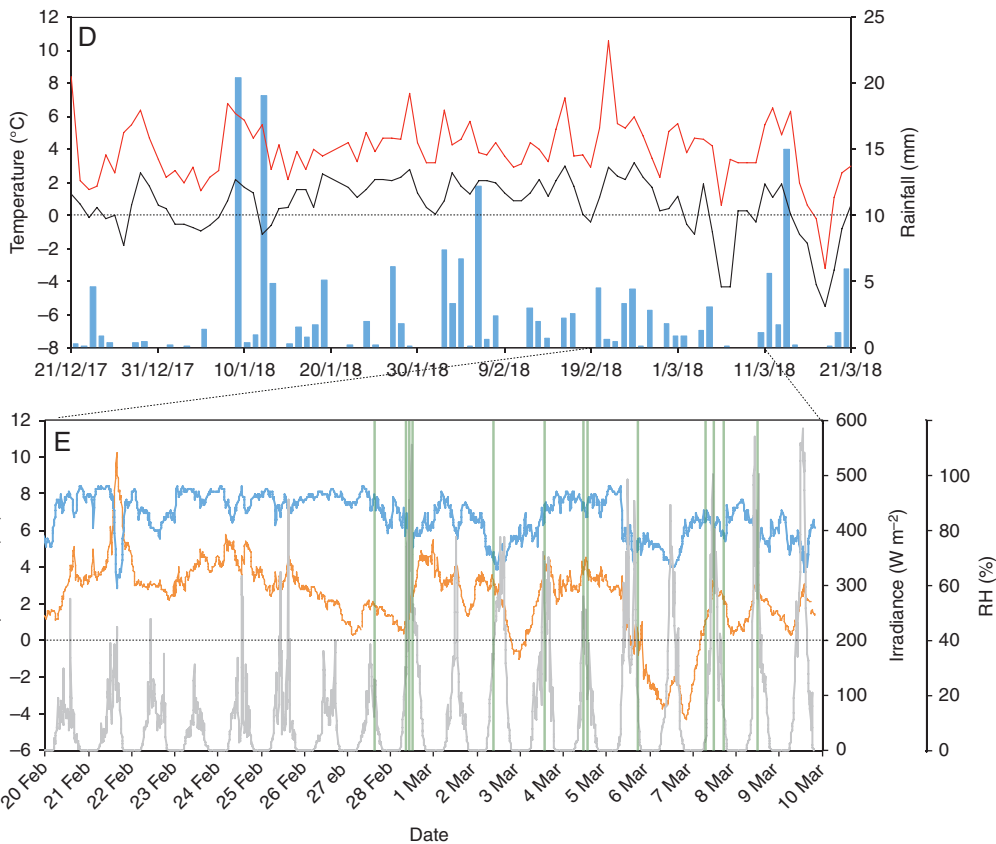


FIG. 1. Collection site: characterization and meteorology. (A) Field site: Argentina Cove in Livingston Island (Maritime Antarctica). (B) Detail of the micro-environment showing the intricate patched carpet formed by *M. tessellata* and *P. crispa*. (C) Gentoo penguin colony (red arrow) close to the studied populations. In panels (A), (B) and (C), blue arrows indicate *M. tessellata* and green arrows indicate *P. crispa*. (D) Meteorological data for the summer of the study obtained from the BAE JCI station: maximum and minimum day temperatures are depicted in red and black, respectively. Blue bars depict cumulative day precipitation. (E) Meteorological data for a temporal window of 1 month including the experimental days (23 February to 6 March). Relative humidity, average temperature and irradiance are presented as blue, orange lines and grey lines, respectively. Vertical green lines highlight the measuring time points for YII (see the Materials and methods section for further details).



*in situ* and *ex situ* measurements, we aimed to address three aspects of photobiont physiology: (1) differences in photosynthetic performance of co-occurring populations of free-living and lichenized *Prasiola*; (2) the extent to which the symbiosis influences water relations in *Prasiola*, including its tolerance of desiccation; and (3) how the association affects survival and performance of *Prasiola* in sub-zero temperatures.

## MATERIALS AND METHODS

### Field site

Co-occurring samples of lichenized and free-living *Prasiola* (Fig. 1A–C) were measured and/or collected on Livingston Island, South Shetland Islands (62°40' S, 60°23' W), near the Spanish Antarctic Research Station Base Antártica Española Juan Carlos I' (BAE JCI) (for further details of the base's location see Laguna-Defior et al., 2016) during summer 2018 (23 February to 6 March). Both *Prasiola* forms were growing on a rocky substrate in Argentina Cove, close to a gentoo penguin (*Pygoscelis papua*) colony (Fig. 1C). Intermediate forms between completely free-living *Prasiola* and the lichen *Mastodia tessellata*, as described by other authors (Huiskes et al., 1997b; Pérez-Ortega et al., 2010), were observed but avoided during field measurements and collections. Measurements took place in austral summer 2017–18, and the weather was characterized by a mean air temperature of 2.3 °C, a range of variation between 10.6 and –5.5 °C, and a small daily thermal amplitude (3.3 °C) (Fig. 1D). Freezing temperatures only occurred at the beginning and end of the season, and were particularly noticeable in March. Rainfall totalled 173 mm during the three summer months (21 December to 21 March), and there was no rain on only one-third of the days (<0.1 mm) (Fig. 1D). The study period (25 February to 10 March) was characterized by two contrasting situations (Fig. 1E). The first week was pretty much comparable to the average summer trend (mean air temperature 2.5 °C, humid and cloudy), while the second week was colder (0.7 °C) and there were many clear sunny periods (Fig. 1E). All meteorological data were kindly provided by the Spanish Agency of Meteorology (AEMET).

### Identity of free-living and lichenized *Prasiola*

Identification of *Prasiola* specimens is usually not a straightforward task due to the reduced number of available taxonomic characters and the presence of cryptic species (Moniz et al., 2012). We used a fragment of the ribulose-1,5-bisphosphate carboxylase/oxygenase large subunit gene (*rbcL*), which has been used in recent studies to infer phylogenetic relationships in the genus (Moniz et al., 2012) and to reconstruct the complex evolutionary history of photobionts associated with *M. tessellata* (Garrido-Benavent et al., 2017). Ten samples (five lichenized, five free-living) were analysed for molecular identification. A small fragment (~1 mm<sup>2</sup>) of sample, cleaned under a dissecting microscope to avoid epiphytic algae, was removed with a razor blade and checked under the light microscope. DNA extraction was carried out using the E.Z.N.A.® Forensic Kit (VWR, Spain) following the manufacturer's instructions.

Amplification was carried out using the primer pair *rbcL*-pras-F and *rbcL*-pras-R (Garrido-Benavent et al. 2018). PCR reactions were performed in a total volume of 15 µL, containing 2 µL of template DNA, 0.5 µL of each primer (10 µM) and 6.5 µL of MyTaq Mix [MyTaq DNA Polymerase (Biolone) and dNTPs]; distilled water was added to reach the final volume. PCR amplifications were performed in an Eppendorf Mastercycler EP gradient S thermal cycler. PCR conditions followed Garrido-Benavent et al. (2018). PCR products were purified using ExoSAP-IT™ PCR Product Cleanup Reagent (ThermoFisher) according to the manufacturer's instructions and sequenced by Macrogen Inc. (Madrid, Spain) using the same primer sets as for PCR amplification. Sequence contigs were assembled using SeqMan v.14 (Lasergene, DNA Star, WI, USA).

### Experimental design

The combination of physiological measurements in the field with physicochemical and biochemical analyses in the BAE JCI and University of the Basque Country (UPV/EHU) laboratories allowed an in-depth ecophysiological comparison of free-living and lichenized forms of *Prasiola*. Alongside the aims of the work, three main experiments were conducted.

Experiment 1. To evaluate the differences in photosynthetic performance of co-occurring populations of lichenized versus free-living specimens of *Prasiola* we combined (1) analyses of photochemical performance and photosynthetic pigment composition under natural conditions in the field with (2) gas exchange measurements of freshly collected wet samples under controlled conditions in the BAE JCI laboratories (Figs 2–4). The assessment of photochemical and photosynthetic pigment adjustments in response to natural irradiance was conducted *in situ* in intact thalli of both species in their natural micro-environment. The actual yield (YII) of photosystem II (PSII), sample temperature and photosynthetic photon flux density (PPFD) were recorded in the field under diverse irradiance conditions and the samples were preserved (fast-dried as described in Esteban et al., 2009) for later analysis of photosynthetic pigments. Three measurements per species and time-point were conducted at a total of 23 time-points with different PPFDs during the days 27 February, 26 February, 2 March, 3 March, 4 March, 5 March, 7 March and 8 March (Fig. 1E, green lines). Further details of chlorophyll fluorescence, gas exchange and pigment analyses are explained below in specific subsections of the Materials and methods section. Experiment 2. This experiment was conducted to evaluate the influence of the symbiosis in water relations of *Prasiola*, including its tolerance of desiccation. For this purpose, pressure–volume (P–V) curves and a desiccation experiment were conducted at the BAE JCI, and an additional set of samples was collected, dried with silica gel and used to assess glass transition temperature ( $T_g$ ) and hydrophobicity of thallus surfaces in the UPV/EHU laboratories (Figs 5 and 6). The desiccation experiment was performed by equilibrating freshly collected free-living and lichenized samples at 10, 50, 80 and 100 % relative humidity (RH) for 48 h in darkness at natural outdoor temperatures (~ +4 °C, data from AEMET station at the BAE JCI for the days of the experiment, 2–4 March 2018; Fig. 1). Using an adaptation of the method

described in López-Pozo *et al.* (2019), incubations were performed in 1-L volume hermetic boxes containing 200 mL of silica gel (to give 10 % RH), MgCl<sub>2</sub> solution (1.87 g of MgCl<sub>2</sub> hexahydrate per mL of Milli-Q water, to get 50 % RH), NaCl saturated solution (80 % RH) or distilled water (100 % RH). The equilibrium RH within the hermetic boxes was tested with an RH and temperature data logger (EL-USB- 2-LCD+; Lascar Electronics, UK). Solutions were adsorbed on a commercial kitchen sponge (Spontex Natura®) separated from the samples by a plastic mesh, and the samples were placed over Petri dishes so that direct contact with the solutions was prevented. Boxes were covered with aluminium foil (to ensure darkness) and located outdoors in the shade to prevent overheating by direct sun exposure. Incubation was conducted for 48 h. To assess the changes in photosynthetic pigments induced by the different incubations, samples were collected after 48 h and immediately frozen in liquid nitrogen. Maximal photochemical efficiency of PSII ( $F_v/F_m$ ) was monitored before incubation and after 48 h. Additionally, a separate set of samples desiccated at 50 % RH were monitored during rehydration at 0, 2, 5, 10, 20, 30 min and 1, 6, 12, 24 and 48 h for detailed analysis of  $F_v/F_m$  recovery. A last set of silica-gel dried samples was preserved for further analyses at the UPV/EHU: P–V curves,  $T_g$  estimation and evaluation of thallus hydrophobicity. Detailed information on these measurements is given in specific subsections of the Materials and methods section.

Experiment 3. In order to assess how the lichen symbiosis affects the survival and performance of *Prasiola* at sub-zero temperatures, a controlled freezing experiment was conducted in the BAE JCI laboratories and a second sample set was used for the assessment of freezing temperature at the UPV/EHU laboratories (Fig. 7). For the freezing experiment, freshly collected wet samples were acclimated to darkness for 12 h and subsequently incubated at –20 °C for 48 h. Changes in photosynthetic pigments were analysed before and after freezing, and  $F_v/F_m$  was monitored during incubation at –20 °C and during re-warming at +20 °C. The experiment was performed in darkness. Further details of the assessment of ice nucleation temperature are given later in a specific subsection of the Materials and methods section.

Whenever required in any of the experiments, controlled hydration was conducted with distilled water since previous studies showed that *P. crispa* and *M. tessellata* are salt-tolerant but not obligate halophytes, being undamaged by hypo-osmotic water (Jacob *et al.*, 1991; Smith and Gremmen, 2001a).

#### Chlorophyll fluorescence

Two types of measurements were conducted with a portable modulated Plant Stress Kit Fluorometer (PSKF, Opti-Sciences, Hudson, NH, USA): YII measurements in the field and  $F_v/F_m$  in the BAE JCI laboratory. The maximum Chl *a* fluorescence under solar radiation ( $F_m'$ ) was induced with a saturating pulse of 0.8 s and 7000  $\mu\text{mol m}^{-2} \text{s}^{-1}$ . The actual efficiency of PSII (YII) was estimated as  $\text{YII} = (F_m' - F_s)/F_m'$ , where  $F_s$  is the actual Chl *a* fluorescence under solar illumination. The saturation pulses for  $F_m'$  estimation were applied as described by Loriaux *et al.* (2013). Maximal photochemical efficiency of PSII ( $F_v/F_m$ ) was assessed in dark-adapted samples in the laboratory for Experiments 2 and 3.

#### Gas exchange measurements

Net assimilation of CO<sub>2</sub> ( $A_n$ ) was determined by using a GFS-3000 gas exchange system coupled with a fluorometer (IMAGING-PAM; Heinz Walz, Effeltrich, Germany). The blue light source provided by the manufacturer, with maximum emission at 420 nm, was used during fluorescence and gas exchange measurements. Fully hydrated samples ( $n = 4$  or 5) were introduced in a custom-made cuvette consisting of a gasket stuck to a thin piece of polyester cloth. The size of the gasket used equalled that of the chamber, so that proper closure of the chamber was possible and CO<sub>2</sub> leakage was close to zero. A similar sample size was used for all replicates of *M. tessellata* and *P. crispa* (average  $\pm$  s.e.  $3.6 \pm 0.3$  and  $3.6 \pm 0.2 \text{ cm}^{-2}$ , respectively). Fresh weight (FW) and DW were individually recorded for each replicate (*M. tessellata*  $77 \pm 5$  and *P. crispa*  $16 \pm 2 \text{ mg DW}$  on average). The CO<sub>2</sub> concentration was standardized at 400 p.p.m. and RH at 75–85 %, and the flow rate within the chamber was 750  $\mu\text{mol s}^{-1}$ . Sample temperature was set to +20 °C, which has previously shown to be optimal for maximum CO<sub>2</sub> assimilation rate in *M. tessellata* (Smith and Gremmen, 2001b). We recorded  $A_n$  under steady-state conditions when diffusion limitations due to interstitial water were null and the biochemistry was fully adapted to light–temperature (3–5 min). Ten light intensities (0, 20, 40, 75, 165, 370, 580, 922, 1465 and 1855  $\mu\text{mol m}^{-2} \text{s}^{-1}$ ) were set in order to obtain a light curve. If needed, full rehydration of the sample during the light curve was done in order to avoid its desiccation by immersing it in distilled water for 1–2 min and gently removing the excess water with a paper tissue before storing the sample in the cuvette again. The negative  $A_n$  at 0 of irradiance ( $I$ ) was considered the dark respiration value ( $R_d$ ). The maximum light-saturated  $A_n$  ( $A_{sat}$ ) and the apparent quantum efficiency (AQE) were obtained by fitting each light curve to Michaelis–Menten (Ritchie and Prvan, 1996a, b), rational (Smith, 1936), exponential (Goudriaan, 1982) or hyperbolic tangent (Jassby *et al.*, 1976) models by using the Microsoft Excel Solver tool (Lobo *et al.*, 2013). The lowest square sum errors were obtained with the Michaelis–Menten model (eqn 1).

$$A_n = \frac{A_{sat} \cdot I}{A_{sat}/AQE + I} - R_d \quad (1)$$

Calculation of the light compensation point at which  $A_n$  equals zero ( $I_{com}$ ) and the irradiance at which 90 % of the  $A_{sat}$  is achieved ( $I_{sat90}$ ) was done for the Michaelis–Menten model (eqns 2 and 3).

$$I_{com} = \frac{A_{sat} \cdot R_d}{AQE(A_{sat} - R_d)} \quad (2)$$

$$I_{sat90} = \frac{A_{sat}(9A_{sat} + R_d)}{AQE \cdot A_{sat} \cdot R_d} \quad (3)$$

#### Photosynthetic pigment and tocopherol analysis

Photosynthetic pigments and tocopherols were analysed by HPLC following the method described by García-Plazaola and Becerril (1999, 2001) with small modifications. Briefly, ~10 mg DW of thalli was used per replicate and three or four

replicates per treatment and/or time-point for photosynthetic pigment analysis. Samples were immediately frozen in liquid nitrogen in the field after treatment and freeze-dried before analysis. Samples were doubly extracted in 0.25 mL of cold (+4 °C) acetone:water (95:5 v:v) first, and in 0.25 mL of pure acetone second. All acetone solutions were buffered with CaCO<sub>3</sub>. Both supernatants were filtered through a 0.2-µm polytetrafluoroethylene filter (Teknokroma, Barcelona, Spain) before being analysed by HPLC. Tocopherol and pigment detection and quantification were conducted with a scanning fluorescence detector (Waters 474) operating in series with a photodiode array detector (Waters 996; Waters, Milford, MA, USA) (García-Plazaola and Becerril, 1999, 2001). The relative de-epoxidation state of the xanthophyll cycle pigments was estimated as the ratio (antheraxanthin + zeaxanthin)/(violaxanthin + antheraxanthin + zeaxanthin), abbreviated as AZ/VAZ.

#### Water potential measurements

Sample water potentials were determined with a dewpoint hygrometer (WP4; Decagon Devices, Pullman, WA, USA) in the laboratory of the BAE JCI, following a protocol similar to that previously used for bryophytes and lichens (Proctor et al., 1998; Nardini et al., 2013; Petruzzellis et al., 2018). The instrument was calibrated at the beginning of each measurement session using 0.5 M KCl standard solution. The fully hydrated thalli (equilibrated for 24 h at 100 % RH over wet paper) were measured for their initial water potential ( $\Psi$ ) and immediately weighed to determine the initial fresh weight. Samples were left to dry on the laboratory bench at 50 % RH and 22–24 °C, and  $\Psi$  was measured subsequently at different times during dehydration. After each reading, samples were immediately weighed to match each  $\Psi$  value to the corresponding weight. At the end of the measurements, each sample was dried in the oven at 70 °C for 24 h to determine the DW. Absolute and relative water contents (WC, RWC) were then calculated for each sample and time point.

Typical P–V curves were obtained by plotting the 1 – RWC values ( $x$ -axis) against the corresponding  $-1/\Psi$  ( $y$ -axis). Two phases were distinguished during desiccation of samples: in the first phase, small changes in  $\Psi$  occurred with high losses of water from the samples until the turgor loss point (TLP) was reached. In a second phase, which corresponds to values below the TLP, the curve became linear ( $r^2 > 0.98$ ). The  $y$ -axis intercept of the linear portion of the P–V curve is the reciprocal of the full-turgor water potential ( $\Psi_o$ ). The point at which the linear portion of the curve begins to curve upwards towards the  $y$ -axis is the TLP; the points between TLP and the  $y$ -axis provide the data for calculating cell wall elasticity, known as the modulus of elasticity ( $\epsilon$ ). The following parameters were calculated according to Sack et al. (2011): water content at full turgor (saturated water content, SWC, g H<sub>2</sub>O g<sup>-1</sup> DW) Capacitance before turgor loss ( $C_{FT}$ ) and at the TLP ( $RWC_{TLP}$ , %); osmotic potential at full turgor ( $\Psi_o$ , MPa); water potential at the TLP ( $\Psi_{TLP}$ , MPa); and modulus of elasticity ( $\epsilon$ , MPa). Specifically, the water mass at turgor was estimated as the intercept of sample water mass and  $\Psi$  at which  $\Psi$  equals zero. Then, the SWC was calculated as water mass at turgor/DW, and one value was obtained per sample. The RWC was estimated as  $(FW - DW)/$

$(TW - DW) - 100$ , where  $TW - DW$  is water mass at turgor, and several data points were obtained for each sample during the desiccation process.

#### Molecular mobility

Mechanical analyses were conducted on desiccated thalli (equilibrated with silica gel) of lichenized and free-living *Prasiola* in order to estimate how lichenization affects molecular mobility of dry thalli. These measurements provide information about the extent of molecular mobility (and thus the potential enzymatic activity) at a wide range of temperatures (Ballesteros and Walters, 2011). A dynamic mechanical thermal analyser (dma/sdta861e, Mettler Toledo, Greifensee, Switzerland) in the shear mode was used for the mechanical analysis. The method was similar to that described by Fernández-Marín et al. (2013) with the modifications described by Fernández-Marín et al. (2018b). Briefly, measurements from –50 to +150 °C at a heating rate of 2 °C min<sup>-1</sup> were carried out in the dynamic mode. Each sample was scanned twice. Three biological replicates, of ~300 mg DW each, were measured per species. Shear storage modulus ( $G'$ ), shear loss modulus ( $G''$ ) and the loss tangent ( $\tan\delta = G''/G'$ ) were calculated using the Mettler Toledo START software during dynamic mechanical thermal analysis (DMTA) scans. For each biological replicate, the temperature value at the maximum  $\tan\delta$  coincident with the  $\alpha$ -relaxation measured at 1 Hz was considered for  $T_g$  estimation.

#### Hydrophobicity of the thallus surface

The contact angle of droplets of distilled water was measured over thalli equilibrated with silica gel in order to estimate the hydrophobicity of their surface, following a method similar to that previously used for lichens (Hauck et al., 2008). Measurements were conducted with a video-based optical contact angle measuring instrument (OCA 15EC; DataPhysics Instruments, Filderstadt, Germany). Sessile droplets of 3 µL were placed on the upper side of the thalli. The contact angle was estimated with the SCA software for optical contact angle, v.4.4.3. The measuring precision was  $\pm 0.1^\circ$ . Measurements were performed on ten thalli per species at 1 s after contact. Each value was the mean from the optically left and right margins of the water droplet.

#### Determination of ice nucleation (freezing) temperature

The freezing temperature of lichenized and free-living *Prasiola* samples was analysed with a differential scanning calorimeter (DSC 822e; Mettler Toledo, Greifensee, Switzerland) at full turgor in thalli of ~10 mg, following a method similar to that described by Fernández-Marín et al. (2018b). Full-turgor samples were sealed in aluminium pans and characterized under constant liquid nitrogen flow (20 mL min<sup>-1</sup>). First, samples were equilibrated at 0 °C and then cooled at a rate of 0.1 °C min<sup>-1</sup> from 0 to –15 °C. Subsamples of the same set as that used for DSC scans were used to estimate absolute water



content. Before the measurements, the DSC equipment was calibrated with zinc, indium and pure water as standards. All weights were recorded using a Mettler Toledo 0.1-mg precision balance. DSC measurements were performed on at least five thalli per species.

### Statistics

Normal distribution of data was checked with the Kolmogorov–Smirnov test and homogeneity of variances with the Levene test. One-way ANOVA was used to test for differences between lichenized and free-living forms of *Prasiola* in each of the analysed parameters: pigment contents,  $WC$ ,  $F_v/F_m$ ,  $T_g$  and freezing temperature, contact angle, and parameters derived from P–V curves and gas exchange modelling. When data showed heteroscedasticity, the non-parametric Kruskal–Wallis test was used. Statistical analyses were conducted with SPSS v24.0 and significance was accepted at  $\alpha = 0.05$ .

## RESULTS

### Identification of *Prasiola* species

Sequences recovered from free-living and lichenized co-occurring samples of *Prasiola* in Argentina Cove showed that they corresponded to two different species. All sequences gathered from lichenized *Prasiola* were identical, and in BLAST searches (Altschul et al., 1997) 100 % matched *Prasiola* sp., a putative new species previously reported from other lichenized *Prasiola* samples from Antarctica (Garrido-Benavent et al., 2017). Sequences from free-living specimens were almost identical (differing at only five positions) and all matched either 100 or 99 % with *Prasiola crispa* in BLAST searches.

### Photochemistry

Figure 1E shows the meteorological conditions (RH, temperature and, more importantly, irradiance) during the measurements of YII and the collection of samples for the subsequent analyses of photosynthetic pigments and tocopherols. The extent of the study period allowed us to get a detailed picture of the response of photochemical parameters to the environmental constraints, e.g. a wide range of irradiances was covered. Figure 2 shows the average content of photosynthetic pigments and tocopherol of samples that were directly preserved in liquid nitrogen in the field. Lichenized and free-living *Prasiola* did not differ qualitatively in their pigment and tocopherol composition. All major carotenoids typical of green photosynthetic organisms, including  $\alpha$ -carotene ( $\alpha$ -Car), not always present, were found, and  $\alpha$ -tocopherol ( $\alpha$ -Toc) was the only isoform of tocopherol identified in both species. Nevertheless, several differences were found in the quantitative contents of photosynthetic pigments. The free-living *P. crispa* showed a significantly higher content of Chl when expressed in terms of DW, and a significantly lower Chl *a/b* ratio (Fig. 2A, B). The free-living

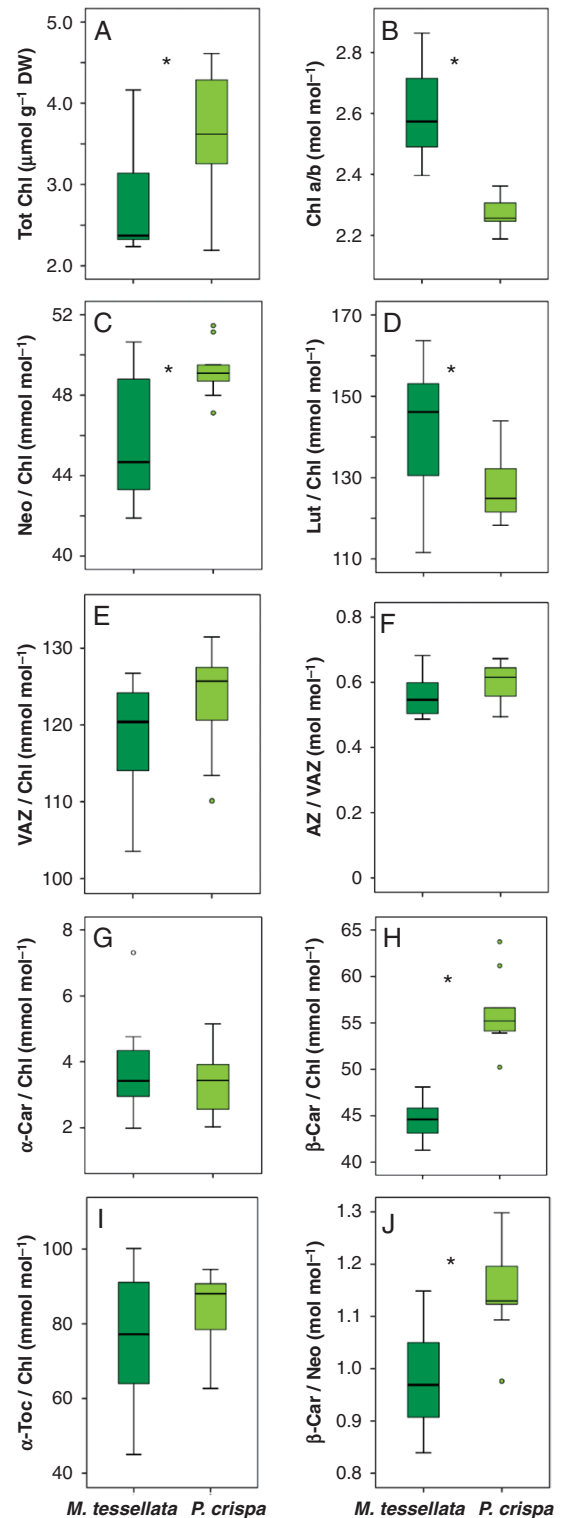


FIG. 2. Boxplots showing the contents of photosynthetic pigment and tocopherol in *M. tessellata* and *P. crispa* thalli collected directly in the field. Boxes cover 50 % of the data; central lines represent the medians and whiskers represent the minimum and maximum values among non-atypical data. Open circles represent outliers. The numbers of reported data are  $n = 8$  for *M. tessellata* and  $n = 9$  for *P. crispa*. Asterisks denote significant differences ( $P < 0.05$ ) between the two species (one-way ANOVA).

*P. crispa* also showed lower thallus mass area (TMA) than *M. tessellata* ( $45 \pm 4$  versus  $224 \pm 27$  g m<sup>-2</sup>, data not shown) and a predominantly mono- or di-stromatic structure with a higher concentration of photosynthetic cells (Supplementary Data Fig. S1). Its lutein (Lut) and  $\beta$ -Car to Chl ratios were higher and its neoxanthin (Neo) to Chl ratio was lower than in the lichenized form (Fig. 2C–H). No significant differences were found in xanthophyll cycle pigments or in  $\alpha$ -Toc content between the two species (Fig. 2E, F, I). Interestingly, the de-epoxidation index of the xanthophyll cycle in these field-sampled thalli was always >0.4 for both species.

An exhaustive sampling of actual photochemical efficiency (YII) during 10 d of measurements was conducted *in situ* (Fig. 3; the exact data points are highlighted as green lines in Fig. 1E). This allowed a detailed characterization ( $n = 122$  data points per species) across a good representation of the natural irradiance range occurring in the microenvironment of both *Prasiola* forms: from 22 to 1679  $\mu\text{mol photons m}^{-2} \text{s}^{-1}$  (Fig. 3A, B). The variability of YII values, particularly at lower irradiances, reflects the potential range displayed for both species as depending, for instance, on water availability (see also Fig. 3C, D). Light responses were photochemically similar between the two species, which showed saturation PPFd at around 600  $\mu\text{mol photons m}^{-2} \text{s}^{-1}$ . Interestingly, free-living *P. crispa* showed higher YII than the lichenized form *Prasiola* sp. at low PPFd, below  $\sim 200$   $\mu\text{mol photons m}^{-2} \text{s}^{-1}$  (Fig. 3A, B). The trend of photosynthetic pigments in response to last-week precipitation and cumulative irradiance was also evaluated (Fig.

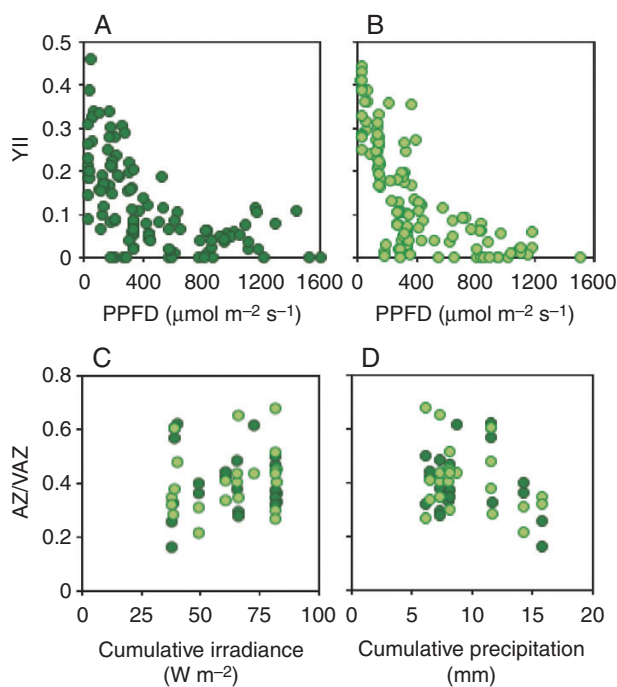


FIG. 3. Photochemical parameters measured in the field under natural irradiance (PPFD) for *M. tessellata* (dark green) and free-living *P. crispa* (light green). Upper panels show the response of actual photochemical efficiency of PSII (YII) to instantaneous irradiance over the thalli of (A) *M. tessellata* and (B) *P. crispa*. Data points are individual measurements ( $n = 122$  per species). Lower panels show changes in the de-epoxidation index of the xanthophyll cycle in response to the last week's cumulative irradiance (C) and precipitation (D). Data points are individual measurements ( $n = 23$  per species).

3C, D). While the two species responded similarly, there was a marked (although not significant) increasing trend in AZ/VAZ in response to higher cumulative irradiance (Fig. 3C) and a decreasing trend in response to higher cumulative precipitation (Fig. 3D).

#### Gas exchange

The value of  $A_{\text{sat}}$  was 47.1 % higher in the free-living alga (Fig. 4B), as a result of increased dark respiration due to the fungal contribution in the lichen ( $R_d$  of  $1.61 \pm 0.12$   $\mu\text{mol CO}_2 \text{ m}^{-2} \text{ s}^{-1}$ , mean  $\pm$  s.e.), than in the free-living *P. crispa* ( $0.47 \pm 0.0712$   $\mu\text{mol CO}_2 \text{ m}^{-2} \text{ s}^{-1}$ ) (Fig. 4C). Net carbon assimilation in response to irradiance was very similar in the two species on a thallus area basis (Fig. 4). By contrast, due to dissimilar TMA and Chl content of the two species (see above), the differences in gas exchange values were accentuated when expressed on a biomass basis (Supplementary Data Figs S2 and S3). Thus,  $A_{\text{sat}}$  was 7-fold higher in *P. crispa* than in *M. tessellata* on a Chl basis (Supplementary Data Fig. S3B) and 9-fold higher on a DW basis (Supplementary Data Fig. S2B). The value of  $R_d$  (on a Chl basis) was not significantly different between the two species (Supplementary Data Fig. S3C) but was higher in *P. crispa* when expressed on a DW basis (Supplementary Data Fig. S2C). The value of  $I_{\text{com}}$  was significantly higher in the lichen ( $78.5 \pm 11.9$  compared with  $12.8 \pm 2.3$   $\mu\text{mol photons m}^{-2} \text{ s}^{-1}$  in *P. crispa*; Fig. 4E) and  $I_{\text{sat}90}$  was accordingly achieved at higher irradiances (Fig. 4D). The two species showed an equal AQE (data not shown). A similar trend occurred when light curves were produced at +10 °C, with an expected displacement towards lower  $I_{\text{com}}$  and  $I_{\text{sat}90}$  (Supplementary Data Fig. S4).

#### Water relations and tolerance of desiccation

Pressure–volume curves and corresponding estimated parameters for thalli of *M. tessellata* and *P. crispa* are shown in Fig. 5. Both osmotic and water potential at turgor were lower in *M. tessellata* than in *P. crispa*:  $\Psi_o = -1.9 \pm 0.8$  versus  $-0.9 \pm 0.0$  MPa; and  $\Psi_{\text{TLP}} = -3.6 \pm 0.1$  versus  $-2.6 \pm 0.1$  MPa, respectively (Fig. 5C, D). Interestingly, the water content at saturation in *P. crispa* ( $\text{SWC} = 2.7 \pm 0.0$  g H<sub>2</sub>O g<sup>-1</sup> DW) was 2-fold higher than in *M. tessellata* ( $1.4 \pm 0.10$  g H<sub>2</sub>O g<sup>-1</sup> DW; Fig. 5E). The modulus of elasticity was also very distinct between the two species, being 3.5-fold higher in *M. tessellata* ( $3.8 \pm 0.0$  MPa) than in *P. crispa* ( $1.1 \pm 0.1$  MPa; Fig. 5F). Remarkably, the TLP occurred at significantly higher RWC in *M. tessellata* ( $\text{RWC}_{\text{TLP}} = 60 \pm 1$  %) than in *P. crispa* ( $42 \pm 1$  %; Fig. 5G). Capacitance at full turgor ( $C_{\text{FT}}$ ) was significantly higher in *M. tessellata*.

Further parameters related to water relations and the capacity to counteract cell dehydration are shown in Fig. 6. Controlled desiccation by equilibrium at three different RHs, in darkness, led to different final water contents (e.g. desiccation extents) of >0.2, around 0.1 and <0.1 g H<sub>2</sub>O g<sup>-1</sup> DW in both species (Fig. 6A). All samples were able to recover their initial  $F_v/F_m$  values after 48 h of rehydration, indicating comparable tolerance of short-term (48 h) desiccation in *Prasiola* sp. and *P. crispa* regardless



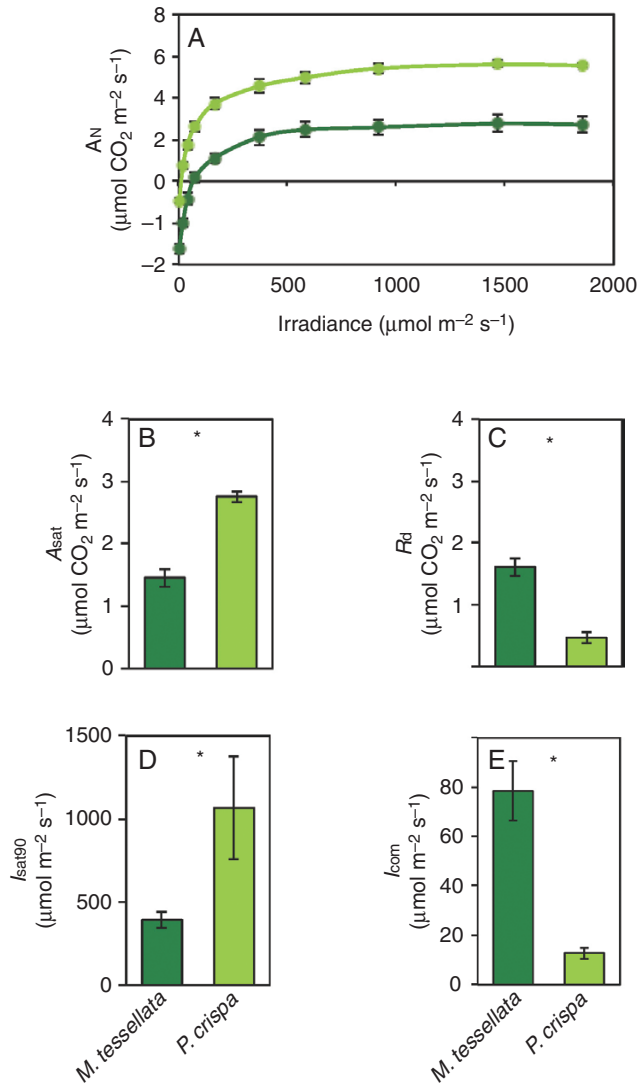


FIG. 4. Gas exchange data for *M. tessellata* (dark green) and *P. crispa* (light green) measured at +20 °C in hydrated samples in the laboratory of the BAE JCI. (A) Light curve of net CO<sub>2</sub> assimilation expressed on a thallus area basis. (B), (C), (D) and (E) depict maximum net assimilation  $A_n$  ( $A_{\text{sat}}$ ), dark respiration ( $R_d$ ), irradiance at which 90 % of  $A_{\text{sat}}$  is achieved ( $I_{\text{sat}90}$ ) and light compensation point ( $I_{\text{com}}$ ), respectively, calculated by Michaelis–Menten curve fitting. Data are mean  $\pm$  s.e. ( $n = 4$  or  $5$ ). Asterisks denote significantly different values ( $P < 0.05$ ).

of the severity of dehydration reached (Fig. 6B). Incubation in darkness induced a slight increase in the de-epoxidation level of both species, although the difference was not significant (Fig. 6C). The mechanical analysis of samples equilibrated at 10 % RH revealed that both species were in the glassy state (e.g. with severely reduced molecular mobility) at ambient temperature (e.g. 4 °C), since their  $T_g$  values were one order of magnitude higher (>40 °C, Fig. 6D). The average  $T_g$  was markedly higher in *M. tessellata* than in *P. crispa* ( $52.2 \pm 4.4$  and  $45.1 \pm 1.0$  °C, respectively) but both *Prasiola* species were able to completely recover photochemical efficiency upon rehydration (Fig. 6E). The contact angle of distilled water droplets over *P. crispa* thalli was on average significantly lower than over *M. tessellata*. This was indicative of significantly higher hydrophilicity in the free-living *P. crispa* (Fig. 6F).

### Freezing tolerance

The course of  $F_v/F_m$  and xanthophyll cycle pigments during a controlled freezing treatment of wet thalli is shown in Figure 7A, B. A slow but progressive decrease in  $F_v/F_m$  was observed during the 48 h of incubation at –20 °C in both species (Fig. 7A). This decrease was remarkably slower in the lichenized *Prasiola* sp., which kept significantly higher values than *P. crispa* during the first 24 h of incubation. In agreement with this, the recovery of  $F_v/F_m$  values during re-warming at +20 °C was also faster in the lichenized *Prasiola* sp., with significantly higher values during the first 30 min. Both species notably recovered their photochemical activity in the extremely short time lapse of 6 h during re-warming to +20 °C: the percentage of the initial value was  $107 \pm 2$  in the lichenized *Prasiola* sp. and  $97 \pm 3$  in *P. crispa* (average  $\pm$  s.e.; Fig. 7A). An increasing trend towards higher de-epoxidation levels was obtained in the thalli at the end of the freezing treatment (around 30 % increase in *M. tessellata* and ~10 % in *P. crispa*), although without statistical significance (Fig. 7B). According to the observed behaviour of  $F_v/F_m$ , the average ice nucleation temperature was significantly lower in the lichen ( $-7.1 \pm 0.4$  °C) than in the free-living *P. crispa* ( $-5.1 \pm 0.4$  °C; average  $\pm$  s.e.) (Fig. 7C; see also Supplementary Data Fig. S4). Thalli of both species subjected to –20 °C in the dry state recovered relatively faster than wet samples during rehydration at +20 °C, with no significant differences between the species (data not shown).

## DISCUSSION

### Lichenized and free-living *Prasiola* populations co-occur in polar regions

The identity of the photobiont of *M. tessellata* as *P. crispa* subsp. *antarctica* and the co-occurrence of free-living and lichenized forms of this species in Antarctica have been long-standing tenets (Huiskes et al., 1997a, b; Lud et al., 2001b). Recently Moniz et al. (2012) resurrected *P. antarctica* Kützinger as an independent species, almost morphologically indistinguishable from *P. crispa* (Lightfoot) Kützinger but molecularly distinct. Garrido-Benavent et al. (2017) studied lichenized *Prasiola* populations from the northern and southern hemispheres, including Antarctica, and concluded that while Tierra del Fuego and most of the Alaskan specimens belonged to the species *Prasiola borealis*, most lichenized *Prasiola* specimens from Antarctica corresponded to an undescribed species, not known so far in a free-living state. Subsequently, Garrido-Benavent et al. (2018) showed in a thorough analysis that *P. borealis* from Tierra del Fuego and *Prasiola* sp. from Antarctica diverged around the middle to the latest Miocene, coinciding with the opening of the Drake Passage. In our study, we found that the two co-occurring *Prasiola* forms belonged to two different species: free-living specimens corresponded to *P. crispa* and lichenized to *Prasiola* sp. The former is a nitrophilic species that usually grows close to penguin rookeries (Graham et al., 2009) and is known from both hemispheres (Moniz et al., 2012). On the other hand, *Prasiola* sp. is, so far, only known in the lichenized form and from Antarctica (Garrido-Benavent et al., 2017, 2018). The fact that co-occurring forms of *Prasiola* do not belong to the same species as previously thought raises the questions of what the

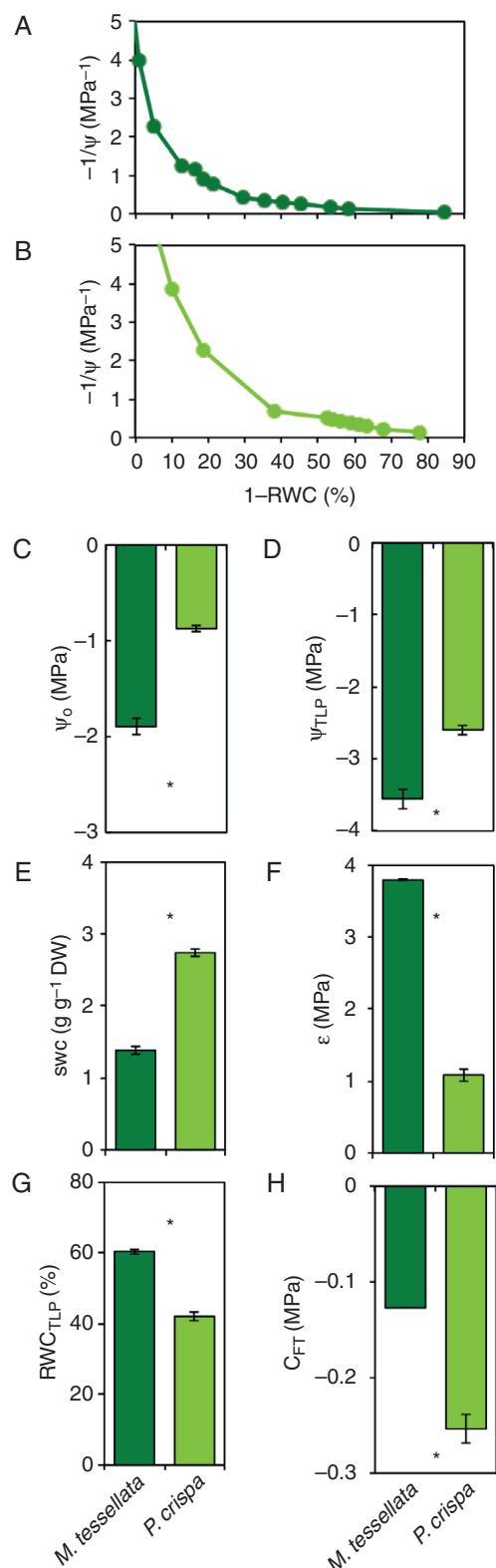


FIG. 5. (A, B) Pressure–volume (P–V) curves of thalli from *M. tessellata* (A) and *P. crispa* (B), showing the changes in inverse water potential ( $1/\psi$ ) as a function of water loss from the thalli (1 – RWC). One representative measurement is shown for each species. (C–H) Selected parameters estimated from the P–V curves (see Materials and methods section for details of the calculations): water potential at full turgor ( $\psi_0$ ), water potential at the turgor loss point ( $\psi_{TLP}$ ), symplastic water content at full turgor (SWC), modulus of elasticity ( $\epsilon$ ), relative water content at turgor loss point (RWC<sub>TLP</sub>) and capacitance before turgor loss ( $C_{FT}$ ). Data are mean  $\pm$  s.e. ( $n = 3$ , for *P. crispa*, 2 for *M. tessellata*). Asterisks denote significant differences among species at  $P < 0.05$ .

niche of free-living *Prasiola* sp. is and whether it does really occur in a free-living state. *Prasiola borealis*, the most common photobiont of *M. tessellata* of Antarctica is known to occur in the free-living state (Garrido-Benavent *et al.*, 2017), and so we expect the same is true for *Prasiola* sp., although it may happen that it occupies a different niche when free-living, as is known to be the case for other photobionts (Sanders *et al.*, 2004).

#### Effect of lichenization on the photosynthetic performance of *Prasiola*

Both lichenized and free-living specimens showed similar photosynthetic performances, with lower net assimilation rates in the lichenized growth form on a thallus area basis (Fig. 4). This is most likely a result of higher energy consumption and respiratory carbon loss deriving from the mycobiont. Dark respiration rates were 4-fold higher than that of the photobiont in its free-living growth form (Fig. 4A, C). The carbon assimilation of *M. tessellata* and different species of *Prasiola* has been reported previously (Smith and Gremmen, 2001a, b; Kang *et al.*, 2013; Holzinger *et al.*, 2017). Nevertheless, and as far as we know, photosynthesis data of both *M. tessellata* and *P. crispa* have only been compared by Huiskes *et al.* (1997b) so far, at non-saturating irradiation and low temperature. In these conditions, *P. crispa* also showed higher  $A_n$  than *M. tessellata*. Photosynthetic capacity of *M. tessellata* was unaffected by low temperatures (from +5 to +20 °C), while  $R_d$  and  $I_{com}$  decreased (Smith and Gremmen, 2001a, b). Although  $A_{sat}$  and  $I_{sat90}$  decreased in the lichenized form (Fig. 4B, D), this should not be interpreted as a lower capacity of the photobiont to consume or deal with excess light, since AQE remained equal to that of the free photobiont and fungal respiration can explain most of the modulation of both parameters. Indeed, the actual irradiance reaching photosynthetic cells in the lichen is very likely reduced by the melanized upper cortex and by the thicker thallus (Supplementary Data Fig. S1). If data are normalized by Chl content, however, the lichenized *Prasiola* appears much less efficient in terms of  $A_N$  (Supplementary Data Fig. S3). This could be explained by (1) the pluri-layered structure of the lichenized algae (Supplementary Data Fig. S1), related to a higher Chl content on a thallus area basis, and (2) by the fungal biomass.

Lichenized and free-living forms of *Prasiola* showed very similar photosynthetic responses to changing light conditions (Fig. 4). In agreement with this, photochemical efficiency (YII) measured in the field responded very similarly to irradiance in *P. crispa* and lichenized *Prasiola* sp. (Fig. 3A). The main difference was observed at low irradiance (e.g. PPFD <200  $\mu\text{mol m}^{-2} \text{s}^{-1}$ ), at which *P. crispa* showed higher YII (Fig. 3A), possibly due to a difference in its alternative sink of electron pathways, since both *P. crispa* and *M. tessellata* presented equal AQE for CO<sub>2</sub> fixation. At higher irradiances (>600  $\mu\text{mol m}^{-2} \text{s}^{-1}$ ) the two species showed similar YII ( $\leq 0.1$ ), but much higher  $I_{sat90}$  was shown by *P. crispa* (Fig. 4D). This could be related to efficient photoprotection mechanisms. *Prasiola crispa* seems to be rather tolerant of UV (Post and Larkum, 1993; Holzinger *et al.*, 2006) and *M. tessellata* has also been shown to be very tolerant even of UV-B (Lud *et al.*, 2001a). Both intensity and quality of irradiance affect photo-inactivation of PSII, and while no data are available for *M. tessellata* so far, a newly identified desiccation-induced protection mechanism that prevents inactivation of the

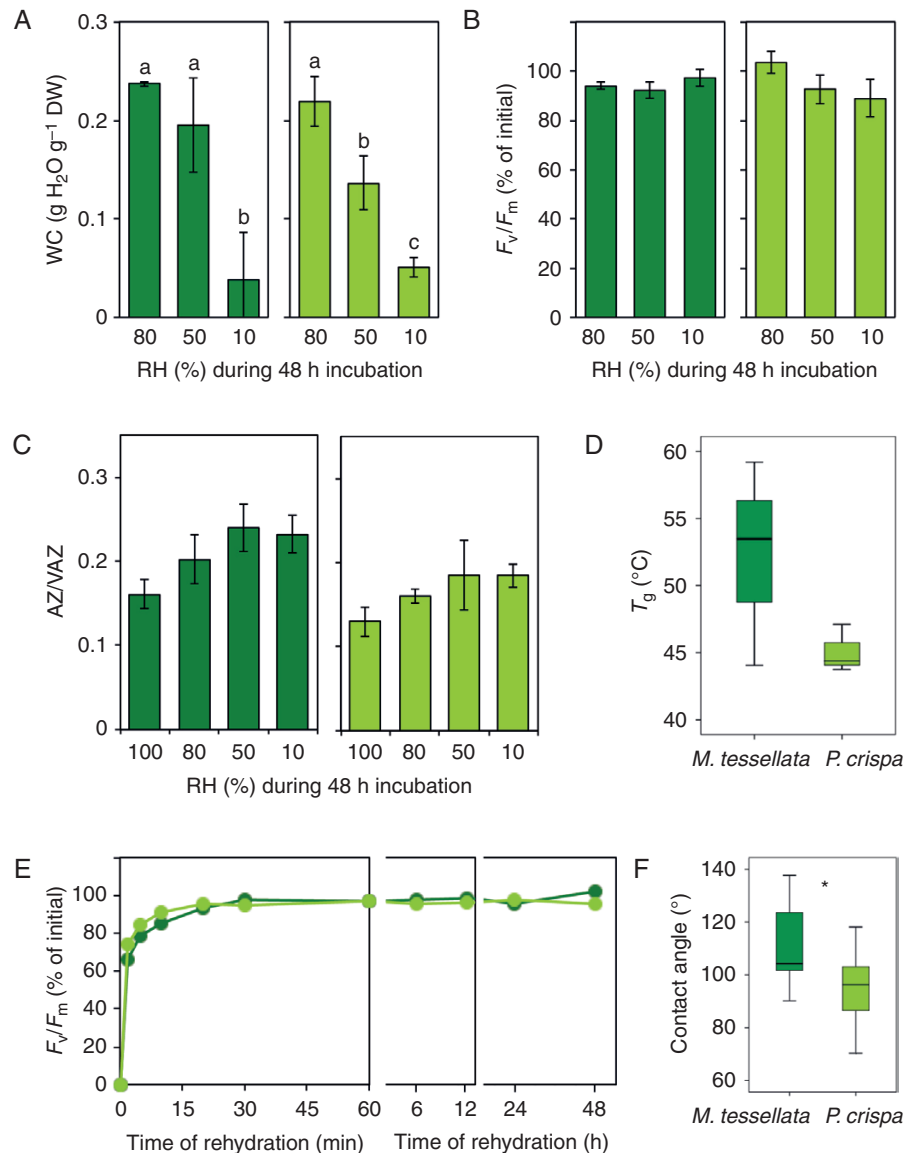


FIG. 6. Physiological, biochemical and physicochemical responses of *M. tessellata* (dark green) and *P. crispa* (light green) under controlled desiccation in darkness. (A) Final water content (WC) at the end of desiccation treatments under different relative humidities (RH). (B) Percentage of  $F_v/F_m$  recovery after desiccation and subsequent hydration. (C) De-epoxidation extent of the xanthophyll cycle pigments (AZ/VAZ) at the end of controlled desiccation. Bars are average  $\pm$  s.e. ( $n = 3$ ). (D) Glass transition temperature ( $T_g$ ) of samples equilibrated at 10% RH ( $n = 3$ ). (E) Recovery kinetics of  $F_v/F_m$  during rehydration of samples previously equilibrated to 50% RH. Data points are average  $\pm$  s.e. ( $n = 6$ ). (F) Static contact angle of a 3- $\mu$ L distilled water drop on thallus surface ( $n = 10$ ). When significant, differences between *P. crispa* and *M. tessellata* are depicted with an asterisk ( $P < 0.05$ ).

oxygen-evolving complex under severely reduced water content has recently been evidenced in Antarctic *P. crispa* (Kosugi et al., 2018).

Chlorophyll content per thallus dry weight was 22.6% lower in *M. tessellata* than in *P. crispa* ( $2.8 \pm 0.2$  versus  $3.6 \pm 0.3 \mu\text{mol g}^{-1}$  DW, average  $\pm$  s.e.; Fig. 2A). The TMA of *M. tessellata* was, on average, 5-fold that of *Prasiola*. Assuming a similar Chl content in free-living and symbiotic *Prasiola*, this would indicate that the mycobiont contributes to only one-fifth of the lichen biomass. This contribution of the mycobiont to the lichen biomass could be even lower if a reduction in the Chl content per area is assumed to be caused by the deterioration of some algal cells with massive penetration of

fungal haustoria (Pérez-Ortega et al., 2010). Interestingly, Chl *a/b*, usually considered a good indicator of light acclimation (the higher the value, the higher the light acclimation) (Esteban et al., 2015), was higher in lichenized *Prasiola* (Fig. 2B). This seems counterintuitive since light-filtering by the fungal tissue should decrease light reaching the photobionts (Solhaug et al., 2010), as it has been described previously that fungal hyphae form a dense network surrounding individual *Prasiola* cells (Pérez-Ortega et al., 2010) and that the outermost layer of the thallus contains melanin (Lud et al., 2001b). This fact could be explained by the preference of *M. tessellata* for more exposed microhabitat or to intrinsic differences between the free-living and symbiotic *Prasiola* species. The latter scenario could also



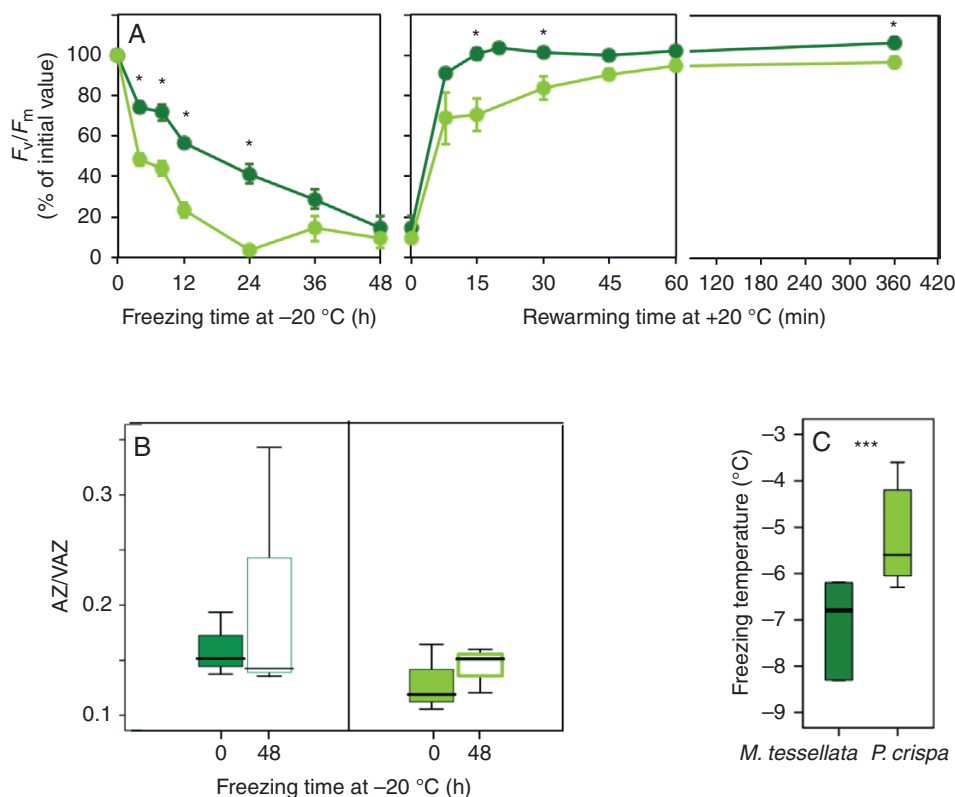


FIG. 7. Physiological and physicochemical parameters of hydrated thalli from *M. tessellata* (dark green) and *P. crispa* (light green) subjected to controlled freezing. (A) Kinetics of  $F_v/F_m$  during freezing (incubation at  $-20^{\circ}\text{C}$ ) and subsequent thawing at  $+20^{\circ}\text{C}$ . Data points are average  $\pm$  s.e. ( $n = 6$ ). (B) De-epoxidation level of xanthophyll cycle before and after 48 h of incubation ( $n = 3$ ). (C) Freezing temperature ranges obtained from onset temperatures of exothermic peak recorded with differential scanning calorimetry during cooling scan ( $n = 6$ ; see Supplementary Data Fig. S5 for representative examples of the scans). When significant, differences between *P. crispa* and *M. tessellata* are depicted with an asterisk ( $P < 0.05$ ).

explain the existence of significant differences in the ratios to Chl of some carotenoids, such as  $\beta$ -Car, Lut and Neo (Fig. 2). Although not evaluated in this work, the ultrastructure of the plastid is very similar in the free-living *Prasiola crispa* (Holzinger et al., 2006) and the lichenized form *M. tessellata* (Pérez-Ortega et al., 2010). Very few studies have dealt with the composition and dynamics of photosynthetic pigments and tocopherol in lichens generally (Demmig-Adams et al., 1990; Kranner et al., 2003; Fernández-Marín et al., 2010; Míguez et al., 2017), and these are virtually unknown at latitudes  $>60^{\circ}$  except for a couple of Antarctic lichen species (Lud et al., 2001a; Strzalka et al., 2011; Sadowsky and Ott, 2012). Our data reveal higher  $\alpha$ -Toc/Chl ratios (around 4-fold) than those found in temperate lichen species (Kranner et al., 2003), which could be a species-specific trait or the combined consequence of age and stress-related factors (Lizarazo et al., 2010). HPLC analyses also revealed that relatively high AZ/VAZ values are maintained continuously in the field in both species, with low re-epoxidation during nights (Figs 1D and 2F). These elevated AZ/VAZ values decreased only after several consecutive days of low irradiance, rain or both (Fig. 3B). Nevertheless, the capacity for faster re-epoxidation of xanthophyll cycle pigments was demonstrated, as samples artificially kept in darkness at high RH showed an AZ/VAZ value of 0.15 (Figs 6C and 7B), a value typical of dark-adapted non-stressed photosynthetic

organisms (Verhoeven et al., 1998). A similar lack of night relaxation of the xanthophyll cycle at high latitudes has been observed during summer in the case of other terrestrial photosynthetic organisms (Fernández-Marín et al., 2018a, 2019), probably indicating an exacerbated de-epoxidation of the cycle under a long photoperiod ( $>12$  h light).

Since lichenization has a tremendous effect in terms of carbon economy for the photobiont, the benefit of the symbiosis could be superior resistance to environmental stress. To test this hypothesis, water relations, desiccation and freezing tolerance were studied in more detail.

#### Water relations and tolerance of desiccation in free-living versus lichenized *Prasiola*

New methodological approaches are providing new perspectives on the ecophysiological interpretation and understanding of water relations in lichens (Nardini et al., 2013; Bacior et al., 2017; Petruzzellis et al., 2018). Compared with other lichen species, *M. tessellata* showed relatively low (very negative)  $\Psi_{\text{TLP}}$  and cell wall elasticity (i.e. high  $\epsilon$ ) (Nardini et al., 2013). In agreement with Petruzzellis et al. (2018), who compared isolated photobionts with their lichenized forms, in our study *P. crispa* samples showed higher cell wall elasticity

(e.g. lower  $\epsilon$ ), higher (less negative)  $\Psi_{\text{TLP}}$  and higher  $\Psi_0$  than *M. tessellata* (Fig. 5). Interestingly, *P. crispa* had higher SWC and lower  $\text{RWC}_{\text{TLP}}$  than the lichen, which, together with the more elastic cell wall, indicates a greater water content range for the free-living algae between saturation and TLPs. Related to this, Baciorek et al. (2017) have recently shown similar hydration kinetics and sorption isotherms for *M. tessellata* and *P. crispa*, with the exception of a larger fraction of loosely bound water in the lichen. The presence of liquid water (rather than vapour) was previously described to be beneficial for high photosynthetic efficiency in *P. crispa* (Kosugi et al., 2010). A high content of easily hydrating pectinic substances in the cell wall has already been proposed as a potential reason behind the water retention properties of *P. crispa* (Jacob et al., 1992). It has been shown recently that the loss of turgor can play a key role in triggering desiccation-related responses at the photobiont cell level (Banchi et al., 2018). In view of this, and based on the differences in water relations found between free-living and lichen-forming species, it would be reasonable to expect different physiological strategies against desiccation.

Our short-desiccation (48 h) approach did not support differences in desiccation tolerance between *M. tessellata* and *P. crispa* (Fig. 6). This terrestrial alga has already been described to be desiccation-tolerant (Kosugi et al., 2010). The authors observed that desiccation induces a strong quenching of Chl fluorescence together with a loss of PSII activity. In agreement with the study of Kosugi et al. (2010) our data showed complete inhibition of  $F_v/F_m$  in the dry state (Fig. 6E). Other species of the genus showed different extents of tolerance of desiccation. The temperate species *P. calophylla*, for example, survives equilibration to 60 % RH for at least 2 h and without alterations in the thylakoidal structure of its chloroplasts (Holzinger et al., 2017), while the arctic *P. stipitata* shows high tolerance of severe desiccation (Kang et al., 2013). This same species, however, shows a deleterious effect upon long-term desiccation (e.g. 30 d) (Kang et al., 2013). Long incubation in darkness also had damaging effects in *P. crispa* equilibrated at different RHs (Jacob et al., 1992), and 96 h of desiccation to 5 % RH induced high mortality in an unidentified *Prasiola* incubated in the presence of light (Davey, 1989). The  $T_g$  value of *M. tessellata* and *P. crispa* in the dry state was around 10 °C higher than previously found for silica-gel-dried mosses (Fernández-Marín et al., 2013) or for resurrection angiosperms equilibrated to 50 % RH (Fernández-Marín et al., 2018b). Although not significant, a clear trend towards higher  $T_g$  was found in *M. tessellata*, which could be related to lower molecular mobility and then slower deteriorative reactions (e.g. ageing) in the long term in the dry state (Fernández-Marín et al., 2013). In the light of the determined  $T_g$  (Fig. 6D) and under the general assumption that tolerance of desiccation of lichen photobionts seems to be enhanced in their lichenized form (Kranner et al., 2005; Kosugi et al., 2009), *M. tessellata* may show better preservation of functional integrity in the dry state at a longer temporal scale. In agreement with this, Huiskes and co-workers found that continuous hydration promotes algal growth while desiccation promotes fungal success within the delicate equilibrium of this symbiosis (Huiskes et al., 1997a).

In summary, our results do not support an effect of lichenization on the desiccation tolerance of *Prasiola* in the short term, although it may have a positive effect upon long-term (several days) desiccation events.

#### Lichenization enhances tolerance of freezing in *Prasiola*

The accumulation of the antioxidant and membrane stabilizer zeaxanthin upon desiccation and upon freezing conditions has been reported in different photosynthetic organisms, including resurrection plants, lichens and intertidal macroalgae (Fernández-Marín et al., 2010, 2011a, b, 2013, 2018b; Verhoeven et al., 2018). Although a trend towards higher AZI/VAZ was observed upon desiccation and at low temperature for *P. crispa* and *M. tessellata* (Figs 6C and 7B, respectively), no significant differences in this ratio were obtained under the experimental conditions used. Even though  $F_v/F_m$  decreased considerably (~90 %) after 48 h of incubation at  $-20$  °C in both species. It is remarkable that this decrease was slower in *M. tessellata*, and only after an incubation time longer than 24 h did the  $F_v/F_m$  drop below 50 % of the initial value (Fig. 7A). By contrast, this happened in the first 6 h of incubation in the free-living *Prasiola* (Fig. 7A). Accordingly, the ice nucleation point was significantly lower in *M. tessellata* than in *P. crispa* (Fig. 7), and 2–3 °C lower than that reported for temperate lichen species growing at high latitudes, such as *Lobaria virens* and *Lobaria pulmonaria* (Solhaug et al., 2018). The lower ice nucleation temperature in *M. tessellata* was in agreement with a slower depression in its photochemical activity along with incubation at  $-20$  °C and with its faster recovery upon thawing when compared with *P. crispa* (Fig. 7). While literature is available about the freezing tolerance of intertidal algae, much less is known regarding the tolerance of freezing in lichens in their hydrated state, and to the best of our knowledge virtually no study has dealt with the effects of lichenization on the enhancement of photobiont fitness under low temperature. Isolated photobionts from Antarctic lichens in the genus *Trebouxia* have been described as highly tolerant of freezing even when artificially isolated from their respective mycobionts (Sadovsky and Ott, 2012). *Prasiola crispa* seems to survive freezing (Jackson and Seppelt, 1995) and some species in the genus show the ability to photosynthesize at low temperatures, down to  $-15$  °C (Becker, 1982). Despite this, in the light of our results it seems that the tolerance of freezing in *Prasiola* can be enhanced in symbiosis with the fungus *M. tessellata* (Fig. 7). Two potential explanations could be argued: (1) morpho-anatomical modifications induced by the presence of fungal hyphae in the lichenized form (see Supplementary Data Fig. S1) and (2) biochemical alterations. In agreement with the former, very recent data on the water behaviour of *M. tessellata* versus *Prasiola* indicate changes in the patterns of ice crystallization induced by both the structure and the biochemistry of the lichenized forms (Baciorek et al., 2019). In agreement with the latter, hardening of the photobiont against environmental constraints (such as desiccation) mediated by metabolic changes (e.g. accumulation of compatible solutes, like arabinol) upon lichenization has been evidenced for some species (Kosugi et al., 2013). In a similar way the contribution of cryoprotectant substances by the mycobiont could be relevant in the protection of the lichenized *Prasiola*.

Although out of the scope of this work, other potential benefits of lichenization to the photobiont, such as the reduced impact of herbivorism or pathogen infection, could be considered in future studies. Interestingly, our data also provide new evidence about how free-living algae can cope with abiotic stress without any protection by the fungal partner. This has also been observed in astrobiological experiments under extreme experimental conditions (Sánchez *et al.*, 2014) highlighting the intrinsic high stress resistance of many lichen photobionts.

### Conclusions

Overall, our work provides new insights into the functioning of the symbiosis established by *Prasiola* sp. and the lichen-forming fungus *M. tessellata* in Antarctica. While lichenization appears to have no positive effect on the photochemical performance of the alga or its tolerance of desiccation (in the short term at least), the symbiosis represents (1) changes in its water relations, (2) a considerable decrease in net carbon uptake (due to fungal respiration and energy consumption) and (3) enhanced tolerance of freezing. The profound impact of lichenization on the carbon balance cannot have a neutral effect; however, there is no clear explanation of why scattered patches of both *Mastodia* and *Prasiola* co-exist in the same microsites (Fig. 1). In the light of our results, enhanced tolerance of low temperature would be a relevant ecological benefit for *Prasiola* upon lichenization. All things considered, whether the overall changes in the functioning of the alga as a consequence of lichenization will be reciprocally beneficial for the symbionts or will favour the single benefit of one of the partners seems to be rather dependent on environmental factors. It has already been reported that warmer winters could be deleterious to freezing-tolerant lichens (Bjerke, 2011) and that the differences in  $A_n$  between *P. crispa* and *M. tessellata* are exacerbated under long-term incubation in the hydrated state (Huiskes *et al.*, 1997b). In a climate change scenario, a rise in temperature that would (1) led to depressed  $A_n$  and (2) reduce the benefits of frost tolerance when lichenized would very likely lead to the spread of the free-living alga to the detriment of the lichen form, with resulting alterations of unknown consequences in Antarctic ecosystems.

### SUPPLEMENTARY DATA

Supplementary data are available online at <https://academic.oup.com/aob> and consist of the following.

Figure S1: details of *M. tessellata* and *P. crispa* anatomy obtained by optical microscopy.

Figure S2: gas exchange data of both species on a DW basis.

Figure S3: gas exchange data of both species on a chlorophyll content basis.

Figure S4: carbon assimilation curve of *P. crispa* and *M. tessellata* measured at +10 °C with a CMS 400 photosynthesis system.

Figure S5: DSC scans of hydrated thalli from *M. tessellata* and *P. crispa* for estimation of freezing temperature.

### ACKNOWLEDGEMENTS

We are deeply thankful for the extraordinary support received at the Spanish Antarctic Research Station BAE JCI from all the staff of the Unidad de Tecnología Marina-UTM, Campaign 2017/2018 and to the AEMET Antarctic group. With particular emphasis we would like to thank to Miki Ojeda and Joan Riba for their outstanding disposition and efficiency in the resolution of difficulties and to José Vicente Albero Molina for kindly providing meteorological data. We also thank our colleague Miquel Nadal for kind help during weighing of samples.

### FUNDING

Spanish Ministry of Economy and Competitiveness (MINECO) and the ERDF (FEDER) funded the projects (CTM2014-53902-C2-2-P, CTM2014-53902-C2-1-P, CTM2015-64728-C2-2-R and CTM2015-64728-C2-1-R) and also funded the ‘Juan de la Cierva-Incorporation’ postdoctoral fellowship (IJCI-2014-22489) to B.F.-M. The Spanish Ministry of Education, Culture and Sport (MECD) supported a predoctoral fellowship (FPU-02054) awarded to A.V.P.-C. The Spanish Ministry of Science, Innovation and Universities supported S.P.-O. through a ‘Ramón y Cajal’ contract (RYC-2014-16784). The Basque Government funded the projects (UPV/EHU IT-1018-16 and UPV/EHU IT-718-13), and a predoctoral fellowship to M.L.-P. Alexander von Humboldt Foundation is gratefully acknowledged for financial support to C.C. via the Feodor Lynen Research Fellowship.

### LITERATURE CITED

- Altschul SF, Madden TL, Schaffer AA, *et al.* 1997. Gapped BLAST and PSI-BLAST: a new generation of protein database search programs. *Nucleic Acids Research* **25**: 3389–3402.
- Asplund J, Wardle DA. 2017. How lichens impact on terrestrial community and ecosystem properties. *Biological Reviews* **92**: 1720–1738.
- Baciór M, Nowak P, Harańczyk H, *et al.* 2017. Extreme dehydration observed in Antarctic *Turgidosculum complicatulum* and in *Prasiola crispa*. *Extremophiles* **21**: 331–343.
- Baciór M, Harańczyk H, Nowak P, *et al.* 2019. Low-temperature immobilization of water in Antarctic *Turgidosculum complicatulum* and in *Prasiola crispa*. Part I. *Turgidosculum complicatulum*. *Colloids and Surfaces B: Biointerfaces* **173**: 869–875.
- Ballesteros D, Walters C. 2011. Detailed characterization of mechanical properties and molecular mobility within dry seed glasses: relevance to the physiology of dry biological systems. *Plant Journal* **68**: 607–619.
- Banchi E, Candotto Carniel F, Montagner A, *et al.* 2018. Relation between water status and desiccation-affected genes in the lichen photobiont *Trebouxia gelatinosa*. *Plant Physiology and Biochemistry* **129**: 189–197.
- Bao T, Zhu R, Li X, Ye W, Cheng X. 2018. Effects of multiple environmental variables on tundra ecosystem respiration in maritime Antarctica. *Scientific Reports* **8**: 1–12.
- Barták M, Váczi P, Hájek J, Smykla J. 2007. Low-temperature limitation of primary photosynthetic processes in Antarctic lichens *Umbilicaria antarctica* and *Xanthoria elegans*. *Polar Biology* **31**: 47–51.
- Becker EW. 1982. Physiological studies on Antarctic *Prasiola crispa* and *Nostoc commune* at low temperatures. *Polar Biology* **1**: 99–104.
- Bjerke JW. 2011. Winter climate change: ice encapsulation at mild subfreezing temperatures kills freeze-tolerant lichens. *Environmental and Experimental Botany* **72**: 404–408.
- Bokhorst S, Convey P, Huiskes A, Aerts R. 2016. *Usnea antarctica*, an important Antarctic lichen, is vulnerable to aspects of regional environmental change. *Polar Biology* **39**: 511–521.
- Candotto Carniel F, Zanelli D, Bertuzzi S, Tretiach M. 2015. Desiccation tolerance and lichenization: a case study with the aeroterrestrial microalga *Trebouxia* sp. (Chlorophyta). *Planta* **242**: 493–505.



- Centeno DC, Hell AF, Braga MR, del Campo EM, Casano LM. 2016. Contrasting strategies used by lichen microalgae to cope with desiccation-rehydration stress revealed by metabolite profiling and cell wall analysis. *Environmental Microbiology* **18**: 1546–1560.
- Colesie C, Büdel B, Hurry V, Green TGA. 2018. Can Antarctic lichens acclimatize to changes in temperature? *Global Change Biology* **24**: 1123–1135.
- Davey MC. 1989. The effects of freezing and desiccation on photosynthesis and survival of terrestrial Antarctic algae and cyanobacteria. *Polar Biology* **10**: 29–36.
- Demmig-Adams B, Iii WWA, Czygan F, Schreiber U, Lange OL. 1990. Differences in the capacity for radiationless energy dissipation in the photochemical apparatus of green and blue-green algal lichens associated with differences in carotenoid composition. *Planta* **180**: 582–589.
- Esteban R, Balaguer L, Manrique E, et al. 2009. Alternative methods for sampling and preservation of photosynthetic pigments and tocopherols in plant material from remote locations. *Photosynthesis Research* **101**: 77–88.
- Esteban R, Barrutia O, Artetxe U, Fernández-Marín B, Hernández A, García-Plazaola JI. 2015. Internal and external factors affecting photosynthetic pigment composition in plants: a meta-analytical approach. *New Phytologist* **206**: 268–280.
- Fernández-Marín B, Becerril JM, García-Plazaola JI. 2010. Unravelling the roles of desiccation-induced xanthophyll cycle activity in darkness: a case study in *Lobaria pulmonaria*. *Planta* **231**: 1335–1342.
- Fernández-Marín B, Míguez F, Becerril JM, García-Plazaola JI. 2011a. Dehydration-mediated activation of the xanthophyll cycle in darkness: is it related to desiccation tolerance? *Planta* **234**: 579–588.
- Fernández-Marín B, Míguez F, Becerril J, García-Plazaola J. 2011b. Activation of violaxanthin cycle in darkness is a common response to different abiotic stresses: a case study in *Pelvetia canaliculata*. *BMC Plant Biology* **11**: 181.
- Fernández-Marín B, Kranner I, Sebastián MS, et al. 2013. Evidence for the absence of enzymatic reactions in the glassy state. A case study of xanthophyll cycle pigments in the desiccation-tolerant moss *Syntrichia ruralis*. *Journal of Experimental Botany* **64**: 3033–3043.
- Fernández-Marín B, Atherton J, Olascoaga B, Kolari P, Porcar-Castell A, García-Plazaola JI. 2018a. When the sun never sets: daily changes in pigment composition in three subarctic woody plants during the summer solstice. *Trees - Structure and Function* **32**: 615–630.
- Fernández-Marín B, Neuner G, Kuprian E, Laza JM, García-Plazaola JI, Verhoeven A. 2018b. First evidence of freezing tolerance in a resurrection plant: insights into molecular mobility and zeaxanthin synthesis in the dark. *Physiologia Plantarum* **163**: 472–489.
- Fernández-Marín B, Gago J, Flexas J, Gulías J. 2019. Plant pigment cycles in the high-Arctic Svalbard. *Polar Biology* **42**: 675–684.
- García-Plazaola JI, Becerril JM. 1999. A rapid high-performance liquid chromatography method to measure lipophilic antioxidants in stressed plants: simultaneous determination of carotenoids and tocopherols. *Phytochemical Analysis* **10**: 307–313.
- García-Plazaola JI, Becerril JM. 2001. Seasonal changes in photosynthetic pigments and antioxidants in beech (*Fagus sylvatica*) in a Mediterranean climate: implications for tree decline diagnosis. *Australian Journal of Plant Physiology* **28**: 225–232.
- Garrido-Benavent I, Pérez-Ortega S, de los Ríos A. 2017. From Alaska to Antarctica: species boundaries and genetic diversity of *Prasiola* (Trebouxiophyceae), a foliose chlorophyte associated with the bipolar lichen-forming fungus *Mastodia tessellata*. *Molecular Phylogenetics and Evolution* **107**: 117–131.
- Garrido-Benavent I, de los Ríos A, Fernández-Mendoza F, Pérez-Ortega S. 2018. No need for stepping stones: direct, joint dispersal of the lichen-forming fungus *Mastodia tessellata* (Ascomycota) and its photobiont explains their bipolar distribution. *Journal of Biogeography* **45**: 213–224.
- Gauslaa Y, Solhaug KA. 1999. High-light damage in air-dry thalli of the old forest lichen *Lobaria pulmonaria* – interactions of irradiance, exposure duration and high temperature. *Journal of Experimental Botany* **50**: 697–705.
- Goudriaan J. 1982. Potential production processes. In: Penning de Vries F, Van-Laar H, eds. *Simulation of plant growth and crop production*. Wageningen: Pudoc, 98–113.
- Graham J, Wilcox L, Graham L. 2009. *Algae*. San Francisco: Pearson Education.
- Guéra A, Gasulla F, Barreno E. 2016. Formation of photosystem II reaction centers that work as energy sinks in lichen symbiotic Trebouxiophyceae microalgae. *Photosynthesis Research* **128**: 15–33.
- Hájek J, Barták M, Hazdrová J, Forbelská M. 2016. Sensitivity of photosynthetic processes to freezing temperature in extremophilic lichens evaluated by linear cooling and chlorophyll fluorescence. *Cryobiology* **73**: 329–334.
- Harańczyk H, Grandjean J, Olech M, Michalik M. 2003. Freezing of water bound in lichen thallus as observed by <sup>1</sup>H NMR. II. Freezing protection mechanisms in a cosmopolitan lichen *Cladonia mitis* and in Antarctic lichen species at different hydration levels. *Colloids and Surfaces B: Biointerfaces* **28**: 251–260.
- Hauck M, Jürgens SR, Brinkmann M, Herminghaus S. 2008. Surface hydrophobicity causes SO<sub>2</sub> tolerance in lichens. *Annals of Botany* **101**: 531–539.
- Heber U, Azarkovich M, Shuvalov V. 2007. Activation of mechanisms of photoprotection by desiccation and by light: poikilohydric photoautotrophs. *Journal of Experimental Botany* **58**: 2745–2759.
- Heber U, Bilger W, Türk R, Lange OL. 2010. Photoprotection of reaction centres in photosynthetic organisms: mechanisms of thermal energy dissipation in desiccated thalli of the lichen *Lobaria pulmonaria*. *New Phytologist* **185**: 459–470.
- Holzinger A, Karsten U, Lütz C, Wiencke C. 2006. Ultrastructure and photosynthesis in the supralittoral green macroalga *Prasiola crispa* from Spitsbergen (Norway) under UV exposure. *Phycologia* **45**: 168–177.
- Holzinger A, Herburger K, Blaas K, Lewis LA, Karsten U. 2017. The terrestrial green macroalga *Prasiola calophylla* (Trebouxiophyceae, Chlorophyta): ecophysiological performance under water-limiting conditions. *Protoplasma* **254**: 1755–1767.
- Huiskes A, Gremmen N, Francke J. 1997a. The delicate stability of lichen symbiosis: comparative studies on the photosynthesis of the lichen *Mastodia tessellata* and its free-living phycobiont, the alga *Prasiola crispa*. In: Battaglia B, Valencia J, Walton D, eds. *Antarctic communities. Species, structures and survival*. Yerseke, The Netherlands: Cambridge University Press, 234–240.
- Huiskes A, Gremmen N, Francke J. 1997b. Morphological effects on the water balance of Antarctic foliose and fruticose lichens. *Antarctic Science* **9**: 36–42.
- Jackson AE, Seppelt RD. 1995. The accumulation of proline in *Prasiola crispa* during winter in Antarctica. *Physiologia Plantarum* **94**: 25–30.
- Jacob A, Kirst GO, Wiencke C, Lehmann H. 1991. Physiological responses of the Antarctic green alga *Prasiola crispa* ssp. *antarctica* to salinity stress. *Journal of Plant Physiology* **139**: 57–62.
- Jacob A, Kirst GO, Wiencke C, Lehmann H. 1992. Physiology and ultrastructure of desiccation in the green alga *Prasiola crispa* from Antarctica. *Botanica Marina* **35**: 297–304.
- Jassby AD, Platt T, Jassby AD. 1976. Mathematical formulation of the relationship between photosynthesis and light for phytoplankton. *Limnology and Oceanography* **21**: 540–547.
- Kang EJ, Serosati RA, Garbary DJ. 2013. Physiological ecology of photosynthesis in *Prasiola stipitata* (Trebouxiophyceae) from the Bay of Fundy, Canada. *Phycological Research* **61**: 208–216.
- Kappen L. 1989. Field measurements of carbon dioxide exchange of the Antarctic lichen *Usnea sphacelata* in the frozen state. *Antarctic Science* **1**: 31–34.
- Kappen L. 2000. Some aspects of the great success of lichens in Antarctica. *Antarctic Science* **12**: 314–324.
- Kappen L, Lange OL. 1972. Die Kälteresistenz einiger Makrolichenen. *Flora* **161**: 1–29.
- Kosugi M, Arita M, Shizuma R, et al. 2009. Responses to desiccation stress in lichens are different from those in their photobionts. *Plant and Cell Physiology* **50**: 879–888.
- Kosugi M, Katashima Y, Aikawa S, et al. 2010. Comparative study on the photosynthetic properties of *Prasiola* (Chlorophyceae) and *Nostoc* (Cyanophyceae) from Antarctic and non-Antarctic sites. *Journal of Phycology* **46**: 466–476.
- Kosugi M, Miyake H, Yamakawa H, et al. 2013. Arabitol provided by lichenous fungi enhances ability to dissipate excess light energy in a symbiotic green alga under desiccation. *Plant and Cell Physiology* **54**: 1316–1325.
- Kosugi M, Shizuma R, Moriyama Y, et al. 2014. Ideal osmotic spaces for chlorobionts or cyanobionts are differentially realized by lichenized fungi. *Plant Physiology* **166**: 337–348.

- Kosugi M, Maruo F, Inoue T, et al. 2018. A comparative study of wavelength-dependent photoinactivation in photosystem II of drought-tolerant photosynthetic organisms in Antarctica and the potential risks of photoinhibition in the habitat. *Annals of Botany* 122: 1263–1278.
- Kranner I. 2002. Glutathione status correlates with different degrees of desiccation tolerance in three lichens. *New Phytologist* 154: 451–460.
- Kranner I, Zorn M, Turk B, Wornik S, Beckett RP, Batič F. 2003. Biochemical traits of lichens differing in relative desiccation tolerance. *New Phytologist* 160: 167–176.
- Kranner I, Cram WJ, Zorn M, et al. 2005. Antioxidants and photoprotection in a lichen as compared with its isolated symbiotic partners. *Proceedings of the National Academy of Sciences of the USA* 102: 3141–3146.
- Kranner I, Beckett R, Hochman A, Nash TH. 2008. Desiccation-tolerance in lichens: a review. *The Bryologist* 111: 576–593.
- Ladrón de Guevara M, Gozalo B, Raggio J, Lafuente A, Prieto M, Maestre FT. 2018. Warming reduces the cover, richness and evenness of lichen-dominated biocrusts but promotes moss growth: insights from an 8 yr experiment. *New Phytologist* 220: 811–823.
- Laguna-Defior C, Pintado A, Green TGA, Blanquer JM, Sancho LG. 2016. Distributional and ecophysiological study on the Antarctic lichens species pair *Usnea antarctica/Usnea aurantiaco-atra*. *Polar Biology* 39: 1183–1195.
- Lizarazo K, Fernández-Marín B, Becerril JM, García-Plazaola JI. 2010. Ageing and irradiance enhance vitamin E content in green edible tissues from crop plants. *Journal of the Science of Food and Agriculture* 90: 1994–1999.
- Lobo F de A, de Barros MP, Dalmagro HJ, et al. 2013. Fitting net photosynthetic light-response curves with Microsoft Excel – a critical look at the models. *Photosynthetica* 51: 445–456.
- López-Pozo M, Flexas J, Gulias J, et al. 2019. A field portable method for semi-quantitative estimation of dehydration tolerance of photosynthetic tissues across distantly related land plants. *Physiologia Plantarum* doi: 10.1111/ppl.12890.
- Loriaux SD, Avenson TJ, Welles JM, et al. 2013. Closing in on maximum yield of chlorophyll fluorescence using a single multiphase flash of saturating intensity. *Plant, Cell and Environment* 36: 1755–1770.
- Lud D, Huiskes A, Moerdijk T, Rozema J. 2001a. The effects of altered levels of UV-B radiation on an Antarctic grass and lichen. *Plant Ecology* 154: 89–99.
- Lud D, Huiskes A, Ott S. 2001b. Morphological evidence for the symbiotic character of *Turgidoscolum complicatulum* Kohlm. & Kohlm. (= *Mastodia tessellata* Hook.f. & Harvey). *Symbiosis* 31: 141–151.
- Míguez F, Fernández-Marín B, Becerril JM, García-Plazaola JI. 2017. Diversity of winter photoinhibitory responses: a case study in co-occurring lichens, mosses, herbs and woody plants from subalpine environments. *Physiologia Plantarum* 160: 282–296.
- Moniz MJB, Rindi F, Novis PM, Broady PA, Guiry MD. 2012. Molecular phylogeny of Antarctic *Prasiola* (Prasiolales, Trebouxiophyceae) reveals extensive cryptic diversity. *Journal of Phycology* 48: 940–955.
- Muggia L, Vancurova L, Škaloud P, Peksa O, Wedin M, Grube M. 2013. The symbiotic playground of lichen thalli – a highly flexible photobiont association in rock-inhabiting lichens. *FEMS Microbiology Ecology* 85: 313–323.
- Nardini A, Marchetto A, Tretiach M. 2013. Water relation parameters of six *Peltigera* species correlate with their habitat preferences. *Fungal Ecology* 6: 397–407.
- Nowak P, Harańczyk H, Kijak P, et al. 2018. Bound water behavior in *Cetraria aculeata* thalli during freezing. *Polar Biology* 41: 865–876.
- Ochyra R, Lewis Smith RI, Bednarek-Ochyra H. 2008. *The illustrated moss flora of Antarctica*. Cambridge: Cambridge University Press.
- Ørstedal DO, Lewis Smith RI. 2001. *Lichens of Antarctica and South Georgia*. Cambridge: Cambridge University Press.
- Pavlova E, Kuzmin A, Pozdnyakov N, Maslov A. 2017. 15N – nitrate uptake and nitrogen exchange in the bionts of the lichen *Parmelia sulcata*. *Symbiosis* 72: 117–121.
- Peat HJ, Clarke A, Convey P. 2007. Diversity and biogeography of the Antarctic flora. *Journal of Biogeography* 34: 132–146.
- Pérez-Ortega S, de los Ríos A, Crespo A, Sancho LG. 2010. Symbiotic lifestyle and phylogenetic relationships of the bionts of *Mastodia tessellata* (Ascomycota, *Incertae Sedis*). *American Journal of Botany* 97: 738–752.
- Pérez-Ortega S, Miller KA, de los Ríos A. 2018. Challenging the lichen concept: *Turgidoscolum ulvae* (Verrucariaceae) represents an independent photobiont shift to a multicellular blade-like alga. *The Lichenologist* 50: 341–356.
- Petruzzellis F, Savi T, Bertuzzi S, Montagner A, Tretiach M, Nardini A. 2018. Relationships between water status and photosystem functionality in a chlorolichen and its isolated photobiont. *Planta* 247: 705–714.
- Post A, Larkum AWD. 1993. UV-absorbing pigments, photosynthesis and UV exposure in Antarctica: comparison of terrestrial and marine algae. *Aquatic Botany* 45: 231–243.
- Proctor MCF, Nagy Z, Csintalan Z, Takács Z. 1998. Water-content components in bryophytes: analysis of pressure-volume relationships. *Journal of Experimental Botany* 49: 1845–1854.
- Ritchie RJ, Prvan T. 1996a. A simulation study on designing experiments to measure the  $K_m$  of Michaelis-Menten kinetics curves. *Journal of Theoretical Biology* 178: 239–254.
- Ritchie RJ, Prvan T. 1996b. Current statistical methods for estimating the  $K_m$  and  $V_{max}$  of Michaelis-Menten kinetics. *Biochemical Education* 24: 196–206.
- Sack L, Pasquet-Kok J, PrometheusWiki contributors. 2011. Leaf pressure-volume curve parameters. *PrometheusWiki*. [http://prometheuswiki.org/tiki-pagehistory.php?page=Leaf\\_pressure-volume\\_curve\\_parameters&preview=16](http://prometheuswiki.org/tiki-pagehistory.php?page=Leaf_pressure-volume_curve_parameters&preview=16)
- Sadowsky A, Ott S. 2012. Photosynthetic symbionts in Antarctic terrestrial ecosystems: the physiological response of lichen photobionts to drought and cold. *Symbiosis* 58: 81–90.
- Sánchez FJ, Meeßen J, Ruiz M, et al. 2014. UV-C tolerance of symbiotic *Trebouxia* sp. in the space-tested lichen species *Rhizocarpon geographicum* and *Circinaria gyrosa*: role of the hydration state and cortex/screening substances. *International Journal of Astrobiology* 13: 1–18.
- Sancho LG, Pintado A, Navarro F, et al. 2017. Recent warming and cooling in the Antarctic Peninsula region has rapid and large effects on lichen vegetation. *Scientific Reports* 7: 5689.
- Sanders W, Moe R, Ascaso C. 2004. The intertidal marine lichen formed by the pyrenomycete fungus *Verrucaria tavaresiae* (Ascomycotina) and the brown alga *Petroderma maculiforme* (Phaeophyceae): thallus organization and symbiont interaction. *American Journal of Botany* 91: 511–522.
- Smith E. 1936. Photosynthesis in relation to light and carbon dioxide. *Proceedings of the National Academy of Sciences of the USA* 22: 504–511.
- Smith VR, Gremmen N. 2001a. *Turgidoscolum complicatulum* on sub-Antarctic Marion Island: carbon acquisition response to climate change. *Polar Biology* 24: 455–459.
- Smith VR, Gremmen NJM. 2001b. Photosynthesis in a sub-Antarctic shore-zone lichen. *New Phytologist* 149: 291–299.
- Solhaug KA, Larsson P, Gauslaa Y. 2010. Light screening in lichen cortices can be quantified by chlorophyll fluorescence techniques for both reflecting and absorbing pigments. *Planta* 231: 1003–1011.
- Solhaug KA, Chowdhury DP, Gauslaa Y. 2018. Short- and long-term freezing effects in a coastal (*Lobaria virens*) versus a widespread lichen (*L. pulmonaria*). *Cryobiology* 82: 124–129.
- Strzalka K, Szymanska R, Suwalsky M. 2011. Prenyl lipids and pigments content in selected Antarctic lichens and mosses. *Journal of the Chilean Chemical Society* 56: 808–811.
- Veerman J, Vasil'ev S, Paton GD, Ramanauskas J, Bruce D. 2007. Photoprotection in the lichen *Parmelia sulcata*: the origins of desiccation-induced fluorescence quenching. *Plant Physiology* 145: 997–1005.
- Verhoeven AS, Adams WW, Demmig-Adams B. 1998. Two forms of sustained xanthophyll cycle-dependent energy dissipation in overwintering *Euonymus kiautschovicus*. *Plant, Cell and Environment* 21: 893–903.
- Verhoeven A, García-Plazaola JI, Fernández-Marín B. 2018. Shared mechanisms of photoprotection in photosynthetic organisms tolerant to desiccation or to low temperature. *Environmental and Experimental Botany* 154: 66–79.